AD-A188 110 LABORATORY FIRE MODELING 1 WIND-AIDED FLAME SPREAD 2 1/1
WET COAGULATION OF S (U) TRW ELECTRONICS AND DEFENSE
SECTOR REDONDO BEACH CA K L BEACH ET AL 21 NOV 86
UNCLASSIFIED DNA-TR-86-248 DNA001-85-C-0102 F/G 15/6 4 NL

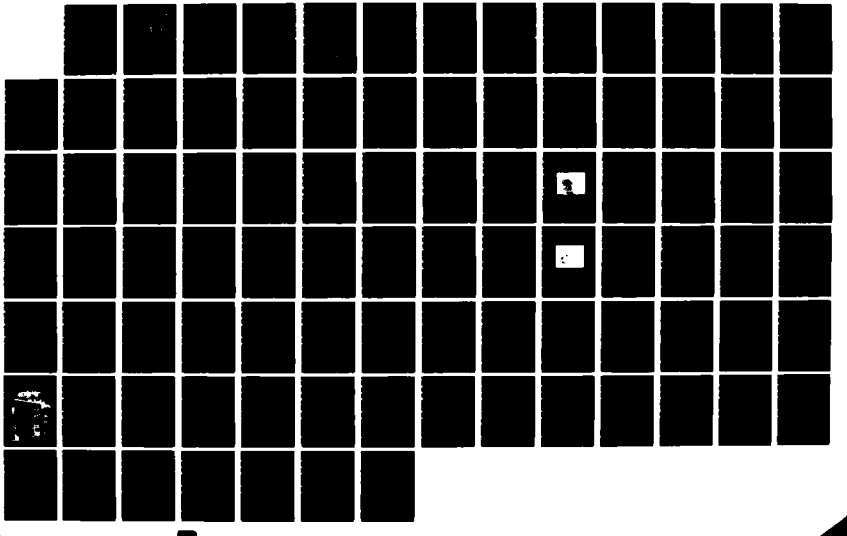

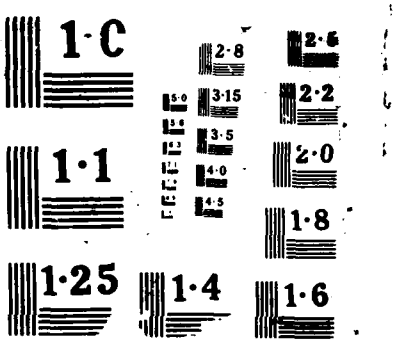
1·C
2·8
2·5
3·15
2·2
3·5
1·1
4·0
2·0
4·5
1·8
1·25
1·4
1·6

(12)

DNA-TR-86-248

LABORATORY FIRE MODELING

1. Wind-Aided Flame Spread
2. Wet Coagulation of Smoke

K. L. Beach, et al.
TRW Electronics and Defense Sector
One Space Park
Redondo Beach, CA 90278

21 November 1986

Technical Report

CONTRACT No. DNA 001-85-C-0102

Approved for public release;
distribution is unlimited.

THIS WORK WAS SPONSORED BY THE DEFENSE NUCLEAR AGENCY
UNDER RDT&E RMC CODE B3450854662 RG RR 00019 25904D.

Prepared for
Director
DEFENSE NUCLEAR AGENCY
Washington, DC 20305-1000

Destroy this report when it is no longer needed. Do not return to sender.

PLEASE NOTIFY THE DEFENSE NUCLEAR AGENCY ATTN: TITL, WASHINGTON, DC 20305 1000, IF YOUR ADDRESS IS INCORRECT, IF YOU WISH IT DELETED FROM THE DISTRIBUTION LIST, OR IF THE ADDRESSEE IS NO LONGER EMPLOYED BY YOUR ORGANIZATION.

CUT HERE AND RETURN

DISTRIBUTION LIST UPDATE

This mailer is provided to enable DNA to maintain current distribution lists for reports. We would appreciate your providing the requested information.

☐ Add the individual listed to your distribution list.

☐ Delete the cited organization/individual.

☐ Change of address.

NAME: _____

ORGANIZATION: _____

OLD ADDRESS	CURRENT ADDRESS
_____	_____
_____	_____
_____	_____

TELEPHONE NUMBER: ( ) _____

SUBJECT AREA(s) OF INTEREST:

_____	_____
_____	_____
_____	_____

DNA OR OTHER GOVERNMENT CONTRACT NUMBER: _____

CERTIFICATION OF NEED-TO-KNOW BY GOVERNMENT SPONSOR (if other than DNA):

SPONSORING ORGANIZATION: _____

CONTRACTING OFFICER OR REPRESENTATIVE: _____

SIGNATURE: _____

Director
Defense Nuclear Agency
ATTN: [redacted] TITL
Washington, DC 20305-1000

Director
Defense Nuclear Agency
ATTN: [redacted] TITL
Washington, DC 20305-1000

UNCLASSIFIED
SECURITY CLASSIFICATION OF THIS PAGE

AD-A188 110

REPORT DOCUMENTATION PAGE

1a. REPORT SECURITY CLASSIFICATION UNCLASSIFIED	1b. RESTRICTIVE MARKINGS
2a. SECURITY CLASSIFICATION AUTHORITY N/A since Unclassified	3. DISTRIBUTION/AVAILABILITY OF REPORT Approved for public release; distribution is unlimited.
2b. DECLASSIFICATION/DOWNGRADING SCHEDULE N/A since Unclassified	
4. PERFORMING ORGANIZATION REPORT NUMBER(S)	5. MONITORING ORGANIZATION REPORT NUMBER(S) DNA-TR-86-248
6a. NAME OF PERFORMING ORGANIZATION TRW Electronics and Defense Sector 6b. OFFICE SYMBOL (If applicable)	7a. NAME OF MONITORING ORGANIZATION Director Defense Nuclear Agency
6c. ADDRESS (City, State, and ZIP Code) One Space Park Redondo Beach, CA 90278	7b. ADDRESS (City, State, and ZIP Code) Washington, DC 20305-1000
8a. NAME OF FUNDING/SPONSORING ORGANIZATION 8b. OFFICE SYMBOL (If applicable) SPTD/Flohr	9. PROCUREMENT INSTRUMENT IDENTIFICATION NUMBER DNA 001-85-C-0102
8c. ADDRESS (City, State, and ZIP Code)	10 SOURCE OF FUNDING NUMBERS PROGRAM ELEMENT NO. 62715H; PROJECT NO. RG; TASK NO. RR; WORK UNIT ACCESSION NO. DH008S22

11. TITLE (Include Security Classification)
LABORATORY FIRE MODELING
1. Wind-Aided Flame Spread; 2. Wet Coagulation Of Smoke

12. PERSONAL AUTHOR(S) Beach, K. L.; Carrier, G. F.; Fendell, F. E.; Gat, N.; Hsu, C. T.; Kwoh, D. S. W.; Lake, B. M.; Wagner, R. N.; Wolff, M. F.

13a. TYPE OF REPORT	13b. TIME COVERED	14. DATE OF REPORT (Year, Month, Day)	15. PAGE COUNT
Technical	FROM 850404 TO 861121	861121	86

16. SUPPLEMENTARY NOTATION
This work was sponsored by the Defense Nuclear Agency under RDT&E RMC Code B3450854662 RG RR 00019 25904D.

17 COSATI CODES		
FIELD	GROUP	SUB-GROUP
13	12	
18	03	

18. SUBJECT TERMS (Continue on reverse if necessary and identify by block number)
Fire Propagation, Precipitation Scavenging, Global Effects, Wind-aided Fire Spread, Wet Coagulation, Flow-assisted Flame Spread

19. ABSTRACT (Continue on reverse if necessary and identify by block number)

Design, construction, instrumentation, and preliminary utilization have been carried out for two laboratory-scale apparati concerned with specific incendiary effects in a thermonuclear aftermath. One apparatus is a fire tunnel dedicated to wind-aided fire propagation across a regular two-dimensional array of discrete polymeric fuel elements (specifically, toothpicks). This work is dedicated to quantifying a local incendiary effect, the rate of fire spread across strewn debris in the presence of an ambient wind. Preliminary findings suggest that the rate of spread increases directly as the square root of the wind speed and inversely as the square root of the fuel loading, for conditions for which spread occurs at all. The other apparatus is a cloud chamber dedicated to characterizing the role of a condensed-water phase on the size distribution and number density of a fire-generated smoke aerosol (as in a capping cloud of a buoyant plume over a vigorous fire). This work is dedicated to helping clarify plausible "initial conditions" for global-effects computer simulation; specifically the work seeks to clarify what fraction of fire-generated smoke

20. DISTRIBUTION/AVAILABILITY OF ABSTRACT ☐ UNCLASSIFIED/UNLIMITED ☒ SAME AS RPT. ☐ DTIC USERS	21. ABSTRACT SECURITY CLASSIFICATION UNCLASSIFIED
22a. NAME OF RESPONSIBLE INDIVIDUAL Sandra E. Young	22b. TELEPHONE (Include Area Code) (202) 325-7042 22c. OFFICE SYMBOL DNA/CSTI

DD FORM 1473, 84 MAR 83 APR edition may be used until exhausted. All other editions are obsolete.

SECURITY CLASSIFICATION OF THIS PAGE
UNCLASSIFIED

19. ABSTRACT (Continued)

undergoes wet coagulation and/or is removed by precipitation, such that the fraction does not reach the stratosphere (or at least not with a size and morphology that suggests that appreciable extinction of incoming solar radiation is effected by that fraction). The aluminum chamber is a constant-mass, batch-type processor of piston-in-cylinder design, with recirculating-liquid refrigeration for wall-temperature control.

PREFACE

The technical suggestions, cooperation, and encouragement of the contract technical monitor Michael Frankel throughout this investigation are very gratefully acknowledged. The participants would also like to thank David Auton and Jacqueline Bell of the Defense Nuclear Agency, as well as Lee Bergerson, Leslie Hromas, and John Kobal of TRW, for helpful assistance. The authors are indebted to Larry Eaton for his contributions on cloud stabilization; to William Finnegan, on wall-temperature-control concepts; to Mark Taylor, on heat-transfer design; and to Ralph Wuerker, on diagnostic optics. They wish to thank Janet Hixson for editing and preparation of the manuscript, and Asenatha McCauley for preparation of the figures.

The division of labor among the participants was as follows. The fire-tunnel-experiment task was carried out by Nahum Gat, Michael Wolff, and Daniel Hsu. The wet-coagulation-experiment-task was carried out by Kenneth Beach, Daniel Kwoh, Bruce Lake, and Richard Wagner. Theoretical work associated with both tasks was carried out by George Carrier, Francis Fendell, Michael Kezerian, and Lawrence Muirhead.

TABLE OF CONTENTS

LIST OF ILLUSTRATIONS

LIST OF ILLUSTR'TIONS (CONTINUED)

SECTION 1

INTRODUCTION

This document reports the status of two laboratory experiments in progress, both concerned with aspects of possible urban incendiary effects in the aftermath of thermonuclear explosions in the troposphere. The concept, design, construction, instrumentation, checkout, and very preliminary data-taking in the apparati are discussed. Further effort is required for utilization of the apparati to furnish the information base which continues to be the ultimate objective of the undertakings.

One experiment is concerned with one aspect of local incendiary consequences of a thermonuclear weapon (Glasstone and Dolan 1977), specifically, fire spread across a regular array of discrete fuel elements under wind-aided conditions. Uncertainty surrounds the extent and pace of flame advance through an urban setting not in disarray owing to blast-caused damage, i.e., still effectively unaltered from its local-fire-code-enforced arrangement. The possibility of fire spread in the undamaged setting prior to effective human countermeasures (and/or prior to arrival of meteorological conditions precluding fire spread) well may depend on the rate of antecedent flame spread through blast-damaged expanses, in general located closer to the hypocenter. Without strong ambient wind, the fire-induced influx of air to the areas first ablaze inhibits spread of flames to further areas. In wildlands it is documented that while the concatenation of hot dry weather, heavy fuel loading, and random ignitions is common, it is only with the coincidence of sustained high winds that exceptionally rapid flame propagation (a "blowup") occurs. In view of these considerations, attention is concentrated here on the less extensively investigated conditions for particularly fast fire advance into previously uninvolved fuel: wind-aided spread. For insight pertinent to fuel distributions, particularly for urban areas blasted to debris but also for normal block-type settings, the persistence and rate of fire spread across a regular "two-dimensional" array of vertically oriented, matchstick-type, discrete fuel elements is measured in a tunnel capable of generating a uniform wind.

The second experiment is concerned with an aspect of a hypothesized global-scale consequence of fires generated in the aftermath of a large number of nearly simultaneous thermonuclear explosions in the lower atmosphere, especially in urban settings (Committee on the Atmospheric Effects...1985). The generation in large-area fires, and the lofting in tall buoyant plumes, of smoky aerosol in general, and carbonaceous soot in particular, is conjectured to be a source of hemispheric-scale reduction of the solar radiation reaching the surface of the earth over a temporal interval persisting for weeks to months. This hemispheric-scale reduction implies darkening during daytimes, and temperature reduction below conventional values. These conjectures are based on the computational results from exercise of global climatological models. Perhaps no input to the calculations is more critical to the results than the initial amount and distribution of soot and aerosol conveyed in discrete mesoscale convection columns to the stratosphere, from which carbonaceous-particulate-deposition rates are exceedingly slow (relative to combined wet-and-dry deposition rates in the conventional troposphere). And perhaps no phenomenon is more uncertain with respect to the significance of its role on the amount of soot reaching the stratosphere for a given attack scenario in a given season than the process of wet coagulation and precipitation in fire-plume-capping (or even other intercepted) clouds during smoky-aerosol transit of the troposphere. In the presence of cloud droplets, soot particles may coalesce to form fewer, larger particles from more numerous, smaller particles, such that the roughly one-tenth-micron size characterizing much of the particulate effluent evolving from large fires increases to roughly near-micron size; while the morphology of the particle is of importance with respect to absorption and scattering of light, in general, less extinction of incoming solar radiation (largely concentrated near the visible portion of the electromagnetic spectrum, i.e., wavelengths roughly over the range 0.42 μm to 0.68 μm) is anticipated from the larger agglomerate (Bohren and Brown 1981). Accordingly, a constant-mass, batch-processing, piston-in-cylinder-type cloud chamber with careful wall-temperature control is developed to study the particle-size distribution in a smoky-aerosol/water-vapor-laden mixture. In particular, a before/after comparison of the size distribution of particulates is made by partial withdrawal of the piston to achieve condensation via expansion, and by

subsequent return of the piston to evaporate condensate via compression. Presumably detrainment from clouds, and re-entrainment into clouds, of the particulate phase can be simulated by muliple expansions and compressions; alternatively, such cycling can be reviewed as simply extending the time interval of exposure to cloud conditions, limited in the laboratory by droplet growth and fallout. Of course, it is also possible to undertake rainout-type simulations of wet-precipitation removal of the smoky aerosol, a process that may occur independently of any smoke coagulation (either because the smoky aerosol provides nuclei for formation of large hydrometeors or because the aerosol is captured by falling hydrometeors).

For clarification of the programmatic contribution to be made by laboratory-scale experiments to larger-scale phenomenology, particularly in fire science and technology, it seems pertinent to conclude this brief preface with a terse review of some of the general advantages and limitations of subscale physical simulation. It is obvious that subscale simulation typically omits relevant physical phenomena that enter on the scale of the full-scale event. In the present contexts, the full lifetime of clouds, the role of atmospheric stratification (density change with height), and the electrical charging in clouds are among effects not readily reproduced in a laboratory-scale, wet-coagulation experiment. Similarly, radiative transfer, wind gustiness, and intricate humidity history are among effects not readily reproduced in a laboratory-scale, wind-aided-firespread experiment. Thus, it is clearly indispensable that preliminary insights achieved on the basis of laboratory-scale experiments ultimately be tested on the scale of the event of interest (or on as large a scale as possible, if full-scale testing is proscribed or unfeasible or economically impossible or whatever). The possibility of misuse and abuse of laboratory-scale data by technical or nontechnical people provides, of course, no logical basis by which to preclude subscale testing as a relatively accessible way of rapidly, economically, and accurately pursuing investigation of relevant parametric dependence of key output. This admonition concerning the ultimate indispensable need for large-scale testing to confirm or reject subscale testing will not be reiterated elsewhere in this report; this single statement is intended to suffice.

Actually, what is being advocated is a sequence of experiments on a series of ever-increasing spatial scales, since very-large-scale fire tests tend to be expensive, executed with long intervening intervals, difficult to instrument adequately, hard to repeat to establish error bounds and to indicate reproducibility, and challenging in the sense of achieving the precise conditions desired. The number of test cases presumably decreases with increasing scale, so in general the smaller-scale tests presumably precede the larger-scale tests; in this way, the likelihood of an unproductive larger-scale test (owing to unexpected dynamic range not suited to selected instrumentation, nonperformance of instrumentation, unexpected and hence inadequately probed locales of important behavior, etc.) is reduced because of prior experience gained at a small scale. In fact, in a later-executed, larger-scale test, it may prove feasible to concentrate mainly on the influence of phenomena inaccessible on a smaller scale. Whether any or all of the subscale series of tests occur within the walls of a structure (i.e., in a laboratory) is a detail dependent on the specific context.

Finally, it is desirable that a theoretical model be developed for predictive purposes, especially for problems in which the phenomena of interest occurs on scales for which little or no experimental testing is likely to be available. Of course, such a theoretical model is invested with credibility by demonstration of its predictive capabilities with respect to closely related phenomena on smaller spatial scale. In this sense, development, application, and upgrading ("tuning") of a theoretical model is aided by the rapid availability of much detailed data taken at prespecified conditions via subscale experiments (e.g., including a laboratory-scale experiment). Indeed, precisely because only a subset of the total number of ultimately relevant phenomena may enter significantly at the smallest subscale for which experimental testing is executed, there is the probability that the theoretical model will not be overwhelmed at the outset of its development. Rather, the opportunity for the theoretical model to be evolved in tractable stages (i.e., levels of sophistication) is enhanced. Of course, if the theoretical model is used for prediction at a scale beyond which it has been tested against experimental data,

engineering judgment carefully must be exercised to assess the plausibility of the results of the extrapolation.[1]

These methodological considerations would seem to urge extensive use of subscale (e.g., laboratory-scale) exerimentation in the pursuit of free-burning-fire-related phenomenology early in a program concerned with complicated, large-scale events. The execution of single-shot, unrepeated, large-scale-but-still-subscale tests would seem to be beset with the liabilities of the full-scale event (expense, poorly uncontrolled conditions, unrepeatability, etc.) without the assets (any subscale event is still not the event of interest, and, without an experimental basis for the assessment, not necessarily significantly more informative than a smaller-scale test). The argument that proceeding immediately to a large-scale test permits early "bounding" of the magnitude of an effect seems unconvincing if the test is still subscale.

---

[1]If a theoretical model, probably a so-called hydrocode executed on a high-speed computer, already exists, then the subscale experiment is useul in either of two ways. If the hydrocode is complete and selfcontained, then the results of the subscale experiments serve to challenge the adequancy of the code with multiple, relatively extensive data sets. In the sense that there may be omitted phenomena because of the subscale nature of the phenomena, the success of a hydrocode in such a check is necessary, but not sufficient, for its validation. Alternatively, hydrocode simulations of large-scale events often encounter the well-known problem of significant phenomena occurring on widely disparate spatial scales. While multigridding concepts are emerging, the conventional procedure is to postulate that subgridscale phenomena can be described adequately in terms of large-grid-scale dependent variables; this frequently adopted postulation is referred to as parameterization. Even if such a parameterization exists (and there are no guarantees), it is usually unknown. Thus, the laboratory-scale data may be sufficient in conditions studied, and in details measured within a condition, to permit evolution and testing of a parameterization (e.g., one for the "microphysical" process of wet coagulation, for incorporation in a buoyant-scale hydrocode for aerosol fate during ascent through the troposphere). Without carefully validated parameterizations for subscale proceses believed to be important, a hydrocode is often incapable of meaningful contribution. For instance, wet-coagulation processes could plausibly result in virtually all, or virtually none, of the soot coagulating to form agglomerates that extinguish exceedingly little of the solar radiation. Without validated parameterizations, often hydrocodes merely rephrase one unknown in terms of another, and, without further (preferably experimental) input, can contribute very limited insight and guidance.

SECTION 2

WIND-AIDED FIRE-SPREAD EXPERIMENT

2.0 INTRODUCTION.

The ability to predict the rate of fire spread (given the topography and elevation, the speed of the wind, the humidity, and the temperature of the environment, and given also the loading, the size distribution, and the geometric arrangement, the moisture content, and the exothermicity of the fuel) would be a very useful achievement for assessing incendiary effects in a thermonuclear aftermath for targeting purposes. Attention here is confined to curcumstances for which significant fire spread is to be anticipated: presence of appreciable sustained wind, in combination with heavy dry fuel loading and an ignition source.

For elucidation of the rate of wind-aided flame spread, a laboratory experiment involving fire propagation across a regular two-dimensional array of discrete fuel elements (here, matchsticks) is undertaken in the presence of a steady wind. The priority presently to be given accumulation of experimental data, to guide the development and validation of fire-spread theories, for forest-type and other environments, has been discussed by Emmons (1965). Of course, ultimately a theory is sought as a means to reduce the labor, time, and expense involved in systematic examination of all conceivably relevant parameters, and as an aid to consideration of what guidance laboratory-scale studies may provide for anticipating spread in larger-scale fire events (which may entail spotting-type spread from firebrands, not included here). Attention is restricted to well-defined experimental arrays so that repetition to identify bounds of uncertainty is readily possible, and so that independent corroboration by other experimentalists also is readily possible. Although a fire "jumps" forward discontinuously through discrete-element fuel beds, the spread rate is taken as effectively continuous for the time scales of practical interest.

Fire propagates through a mixed-size array of fuels at the rate at which the thermally thin fuels (i.e., the fuels well described as isothermal) are desiccated and heated to their pyrolysis temperatures. In a forest, for example, in which all combustible matter is roughly of one

general type, the thermally thin fuels are the physically thin fuels, and a general rule of thumb is that leafy matter, together with woody matter with diameter of less than one centimeter, is consumed as the fire-front passes. Thicker fuels, in fact, might act as heat sinks as far as fire-front propagation is concerned, though these fuels may eventually burn (and any thin-fuel char may eventually be oxidized) in the burned-gas region well behind the fire front. Thus, in the simpler earlier experiments to be undertaken here, only thin fuel is present; the role of inert material and thicker fuel may be included in later experiments by distributing noncombustibles in a regular arrangement through the fuel array.

Incidentally, Cheney (1981) suggests that convection associated with the longer-term burning of coarser fuels behind the flame front may constitute an effective barrier to the spread-aiding wind; however, the consumption of wind-retarding shrubs could also reduce an impedance in the fuel bed to the ambient wind. A point worth noting is that, owing to the varying importance of drag by "obstacles", the ambient wind and the wind at the fuel bed may be comparable (as in grasslands) or quite distinct (as in tall forests). Reference to the wind speed in this text is to the ambient value, in the absence of specification to the contrary; however, a major consideration in future work is to quantify the near-fuel-bed decrement in the upstream wind in the current experiment.

Although analyses exist that emphasize the role of convective transfer in preheating fresh fuel for fire spread through matchsticks (e.g., Vogel & Williams 1970), the present work takes radiative transfer from flaming elements to fresh elements to be the primary preheating mechanism in agreement with Emmons (1965) and Emmons & Shen (1971). Van Wagner (1968) infers that 20-30% of the exothermicity from burning goes into radiation for wind-aided wildlands fires, and this more than suffices to meet the preheating needs to sustain fire propagation. Increasing the ambient wind speed can tilt the flame downwind, such that the view factor is increased and preheating is more rapid (Steward et al 1977). Convective heat transfer may become a contributory spread mechanism at high-enough wind speed, but the role of radiation seems primary (Rothermel & Anderson 1966). Reference in this paragraph is to the mechanism responsible for the preponderance of the temperature rise from ambient to pyrolysis temperature (~500 K), not to the

mechanism significant immediately at the front of the flaming (where bulk-gas temperature may reach 1000 K to 1200 K).

A further increase of the wind can blow the buoyant flame over and effect contact ignition. But a still further increase can lead to extinction of burning because the flow rate exceeds the reaction rate, and heat is convected away faster than it is released by exothermic chemical reaction. Whereas forced-convective extinction of diffusion flames is well established for many familiar fuels (liquid hydrocarbon droplets, wooden slabs, etc.), it has not been well documented for laboratory discrete-fuel-element beds, though it has been observed under extremely rapid winds in grasslands (Luke & McArthur 1971, pp. 86-90; Cheney 1981, p. 166), and in crown fires during forest fires in which the shielded surface spread was not blown out (Luke & McArthur 1971, p. 94).

For a finite-length fuel bed, a steady rate of flame propagation may or may not be established after transients associated with ignition die out. One criterion that is prerequisite for a steady flame propagation to be achieved is that a flaming zone of finite thickness is observed. Thus, it is important that the downwind extent of any fuel-bed array be at least half again as long as the fire-front thickness, a thickness not known a priori. Therefore, it is not always evident before an experiment that a steady rate of fire propagation will be attained in any finite-length fuel bed. Incidentally, it is possible that, under some modes of ignition, unsteady rates of spread could well exceed the quasisteady rate of spread that presumably would be achieved for a long-enough uniform fuel bed under constant slope, wind magnitude and direction, etc. Byram et al. (1966) discuss the reassessment of inferences drawn from wind-aided-spread experiments in which steady rate of fire propagation was not achieved.

Nonmonotonic dependence of the rate of fire spread many hold with respect to fuel loading as well as with respect to the wind. For example, Cheney (1981) reports that the spread rate varies linearly with the fuel loading; Thomas (1971) reports that it varies inversely with loading. Again, relating these parametric domains is highly desirable.

It seems worth emphasizing that failure of fire to propagate in a laboratory facility does not mean that the effective firebreak dimension

has been identified for the conditions under examination, because firebrands may be present in the "field". Also, although the fastest rates of spread occur under an aiding wind of not-too-great intensity, it seems worth mentioning that slower but still finite rate of propagation can occur in the absence of ambient wind or even against the wind.

In the cases to be examined here, the mean wind is constant in magnitude and direction and is oriented perpendicular to the leading edge of the two-dimensional fuel array. The information so obtained is applicable to ascertaining the evolution of the fire perimeter in time in a more general context, provided that the quasisteady approximation is adopted. (Explicitly, the instantaneous wind magnitude and direction, not the rate of change of either, is taken to be pertinent for deducing where a fire perimeter is at a later time, given its position at an earlier time.) The component of the wind locally perpendicular to the fire front is the component that aids spread; the component of the wind locally parallel to the fire front does not aid spread. Even in a homogeneous fuel bed subject to line ignition perpendicular to the wind, radiative losses at the lateral edges result in the formation of faster-moving "heads", so the fire front usually does not remain linear; the width of the fuel bed becomes an issue in the presence of such lateral radiative losses. More generally, in wildlands, point ignition(s), fuel inhomogeneity, wind variations, etc., result in the arising of heads. Thus, it seems worth emphasizing the applicability of data gained from two-dimensional, line-fire (or near-line-fire) experiments to predicting the propagation of more general, elliptically-shaped fire fronts.

Increase in the fuel moisture content (which, for thin fibrous fuels, adjusts to the ambient relative humidity relatively quickly, with some variation depending on whether absorptive or desorptive processes are involved) decreases the rate of spread; high-enough moisture content renders ignition and spread unlikely, if not impossible. The role of moisture content (like the role of slope) has been examined in quantitative detail elsewhere (e.g., Luke & McArthur 1971), and attention is here concentrated on the fuel loading and wind. However, it is noted that, whereas the role of moisture content is accounted for below via minor adjustment of the effective heat of combustion, there are other

moisture-associated effects (e.g., longer time to achieve pyrolysis, dilutive effects of much water-vapor release with fuel-vapor release, and alteration of radiation owing to water-vapor bands) which are probably of more consequence.

2.2 SOME CONJECTURES.

2.2.1 Postulation of a Plume-Dominated Domain.

Cheney (1981, pp. 168-169) suggests that strongly wind-aided spread involves the balance of crossflow dynamic pressure and combustion-heat-release rate. Actually, quantification of a plume/crossflow interaction traces back four decades to Rouse, and a key insight in the aerothermochemical context is due to Taylor (see Fleeter et al. 1984). Taylor's conjecture is that there exists a condition of fire spread in which the entrainment requirements of a fire-generated line plume are just met by the crossflow. In this conjecture, the buoyancy-generated updraft and the crosswind U are in balance: if a stronger wind gust occurs, the plume is blown over, whereas if the wind decreases, then the propagation slows, since a weaker updraft suffices to be in equilibrium with the crosswind. Because the updraft is related to the intensity of the buoyant line source (heat per time per depth), and because the intensity in turn is equal to the product of the effective heat of combustion Q (exothermicity, minus heat of desiccation heat and heat of pyrolysis--if any, per mass of fuel), the fuel loading σ (mass of thin fuel per area), and the spread rate v_f (fire-spread speed), it follows that the spread rate increases with increasing wind speed but decreases with increasing fuel loading. Explicitly (Fleeter et al. 1984),

$$v_f = \frac{1}{8\alpha^2} \frac{\rho_\infty c_p T_\infty U^3}{Q g \sigma} . \qquad (1)$$

Here, g is the magnitude of the gravitational acceleration; c_p, ρ_∞ and T_∞ are, respectively, the heat capacity, the density, and the temperature of ambient air; and α is the entrainment constant for a line plume ($\doteq 0.16$). More precisely, in (1), σ denotes the fuel actually burned during fire-front passage; combustion tends to be less efficient as the spread rate increases. Incidentally, Cheney (1981) notes that v_f has been conjectured

to increase linearly, quadratically, and exponentially with the wind, but apparently not cubically.

In (1), the ambient temperature T_∞ may vary typically from 285 K to 320 K and thus alter the duration of the preheating interval from ambient to pyrolysis condition, but in fact the product $\rho_\infty T_\infty \sim p_\infty$ and thus varies at most on the order of 10%. Similarly, even with consideration of desiccative and radiative losses, $Q \doteq 1.8\times10^{11}$ ergs/g and varies on the order of 30% for forest fuels; Q may be twice the cited value for synthetic polymers. However, in wildlands the thin-fuel loading σ easily varies over an order of magnitude, with 0.01 g/cm^2 to 0.1 g/cm^2 lying within the domain of interest. Winds U of interest range from (say) 100 cm/s to 2000 cm/s. Thus, the reported two-to-three orders of magnitude variation in spread rate in v_f in wildlands is preponderantly attributable to σ and (especially) U. This statement seems plausible even if (1) is found to be seriously inadequate.

This plume-dominated mode of propagation, in which radiative transfer from the plume to the downwind fresh fuel is implicitly the mode of preheating to the pyrolysis temperature, might be considered a special circumstance. However, it seems possible that the spread rate increases or decreases to consume fuel as required to maintain the marginal balance, so that the configuration is rather stable. Nevertheless, there must be fuel loadings inhomogeneous enough that the overall mass per area of thin fuel is an insufficient characterization. In the last instance, the discrete nature of the fuel in the form of (say) the spacing between individual fuel elements may enter.[2]

Thus, one objective of experiments is to delineate the range (if any) of crosswind speed U, thin-fuel loading σ, and fuel-element spacing s for which (1) suffices. The model that yields (1) ignores virtually

---

[2]The need under some circumstances to consider the fine scale of the thin-fuel loading arises because there are many ways to achieve even a regular orthotropic discrete-fuel-element arrangement with a particular loading $\sigma = \sigma_1$. (The need to consider <u>sometimes</u> the crystalline structure of a solid in elasticity comes to mind as an analogy.) For a fuel bed of identical vertically-arranged uniformly-spaced square-cross-section matchsticks (of side d and length L, arranged with center-to-center spacing s), the bed porosity $\phi = 1 - (d/s)^2$ and the loading $\sigma = (1 - \phi)\rho_s L$, where ρ_s

completely the details of the downwind fuel preheating and the upwind fuel burnup, and even ignores radiative heat losses from the plume. In the introduction, it already was noted that a head inevitably forms (e.g., from edge-type radiative losses); hence, a line-source plume without radiative losses is an overidealization. Also, for sufficiently sparse arrangement, downwind radiation tends to be more incident on fuel-free regions, so the relation $v_f \sim \sigma^{-1}$ fails long before $\sigma \to 0$. Finally, Taylor himself warns that near-ground decrement in the ambient wind is overlooked in the simplistic theory; furthermore, the use of plume-type entrainment concepts in the flaming zone is also dubious. Thus, the failure of (1) with respect to data cited below evokes no surprise, though such guesses deserve checking out.

For completeness, it is noted that tall buoyant columns usually are associated with long-lived, more slowly spreading conflagrations, in which fire propagates outward against a convectively induced indraft. The fire-front plumes associated with wind-aided spread usually are not of an altitude comparable to the scale height of the troposphere.

2.2.2 Less Explicit Statement of Parametric Dependence.

As implied first by Fons (1946), the necessary criterion for flame propagation is that $t_b > t_i$, where t_b is the time interval for burning of an upwind element and t_i is the time interval required to ignite the neighboring downwind element under the heating from the neighboring upwind element (and possibly others in its proximity). (Although it is nonessential, t_i could be associated with t_p, the time required to bring the fresh element to its pyrolysis temperature, if it be taken that outgassed combustible vapor is invariably ignited.) In any case, it is believed here that attempts at theoretical treatment of the radiative heating of a nonburning element, owing to the burning of a nearby element,

---

[2] (Continued) is the (true) density of the matchstick material. Clearly one might alter d, s, ρ_s, and/or L (while leaving σ invariant) and thereby might alter v_f (for fixed U, fixed moisture content, and fixed slope). For experiments limited to the same type of matchsticks in such regular arrays, variations in σ are achieved by changes in s; then, sensitivity to the discrete nature of the fuel distribution may indeed be masked by the arbitrary adoption of σ instead of s as the key variable. A simple variation is to use matchsticks of the same type (ρ_s,d invariant) but of different length L and spacing s.

lack credibility owing to the idealizations necessarily adopted for tractability. Thus only a general statement of a functional relationship is undertaken; the explicit functional dependence is to be obtained from experimental data, in this less ambitious approach.

Let q be the total heat output of a single fuel element. The quantity t_b can also be measured; it depends on the fuel substance (wood, plastic, tar, etc.), on fuel-element surface area A, on moisture content of the fuel, etc. Let R be defined as the rate at which heat is absorbed by an adjacent, downwind, still-unignited element. Then, one may hypothesize for R that a separable dependence on key parameters exists:

$$R = \left[g'\left(\frac{q}{t_b}\right)\right]\left[f'(s)\right]\left[h'(A)\right]\left[j'(U)\right] , \tag{2}$$

where s is the spacing of elements; g',f',h',j' are functions to be identified; and other factors (such as fuel-element thickness) may have been inappropriately omitted from the right-hand side of (2). It can be hypothesized further that

$$t_i = \text{fnc}(R) . \tag{3}$$

One might just as well dispense with R and define

$$t_i = g\left(\frac{q}{t_b}\right) f(s)\ h(A)\ j(U), \tag{4}$$

where f,g,h,j can be inferred from experiments in which t_i is also measured. If

$$v_f = s/t_i , \tag{5}$$

then observation of v_f implies t_i, and vice versa.[3] The potential usefulness of (4) and (5) is that, if f,g,h,j were identified adequately from earlier testing, one could not only predict v_f, but also might gain insight into spread-rate-controlling mechanism(s).

2.3 REVIEW OF THE LITERATURE.

3.1.1 Studies Not Addressing Propagation.

A number of theoretical investigations exist in which the interaction of a line fire and a crosswind is examined (e.g., Gostintsev & Sukhanov 1978a, 1978b, 1979; Luti 1980, 1981; Grishin et al. 1985). Whatever the physical validity of these models, they do not pursue the matter of key interest here: the rate of fire propagation. The experimental counterparts of these theoretical investigations involve experiments in which a line fire of fixed position is subjected to a crosswind (e.g., Thomas 1963; Putnam 1965); again, without comment on the validity of the conclusions, these seemingly related works are not relevant to present objectives.

3.1.2 Flame Spread in the Absence of an Ambient Wind.

Since attention here is focussed on line-fire-type spread across discrete-fuel-element arrays in the presence of an ambient wind, no exhaustive review of propagation in still air is attempted; however, a few of the many published works are noted.

Among the first efforts at reproducible laboratory tests with a regular, well-defined, noncontinuous fuel are those due to Fons and collaborators with woodcribs (see Fons et al. 1963); unfortunately, some of the publications give insufficient data to permit characterization of the fuel loading. Fang & Steward (1969) have conveniently collected much of the data on pine-needle and pine-stick beds, and have added results of

---

[3] An attempt made to measure t_i and t_b in experiments to be discussed below, by visual observation and a handheld stop watch, proved unsuccessful for conditions of rapid spread, for which the flaming front is relatively thick; the use of thermocouples seems advisable. The quantity t_b may be assigned approximate values by the burning of isolated fuel elements. If the burn time t_b is independent of wind speed U for a given type of fuel element (A held fixed), then the spread rate is a function of spacing s and wind speed U only, for thin fuel elements. In such circumstances, (2.4) and (2.5) involve precisely the same variables as (2.1), but no explicit functional relation is postulated.

their own on uniform randomly packed fuel beds consisting of poplar-hardwood shavings. The results indicate that the spread rate is relatively independent of fuel loading (mass of fuel per area of bed surface). However, spread rate increases with decreasing humidity (since this implies decreasing moisture content of the fuel, and moisture is evaporated at about 373 K, with the appropriate enthalpy requirement for heat up and phase change, whereas an appreciable pyrolysis of combustible vapor from thin woody fuel tends to occur in the range of 475 K to 675 K). Moreover, the fire-spread rate nearly doubles as the fuel-bed voidage is increased from 0.85 to 0.975. Of course, any such generalities as those just stated are limited to the parameter ranges actually examined, and, in fact, Hottel et al. (1965) have noted that the rate of flame spread increases with fuel loading up to a certain value, and only then becomes invariant with further fuel loading; whereas Hottel et al. (1965) employed shredded newsprint and cut-up computer cards to obtain this results, Steward et al. (1977) noted the same trend in matchstick arrays in which the fuel, spacing, and humidity were held fixed while the length of elements was increased. One may conjecture that the flame-front propagation requires consumption of only a fraction of the fuel present in order to produce the exothermicity required to heat further downwind fuel to pyrolysis and ignition, and thereby to sustain the propagation; the excess fuel loading burns in the aftermath of the fire-front passage (if it burns at all) and does not alter the propagation rate. Indeed, if the "excess" fuel were to alter fire-propagation rate at all, it might be to slow the spread, since it is conceivable that the excess fuel could serve as a heat sink during front passage, as noted earlier. It seems appropriate to note that Steward et al. (1977) also report that, for matchsticks and for 0.25-cm-diameter birch dowels, the flame propagation rate is near maximum over a certain range of element spacings, and falls off very rapidly at both larger and smaller spacings. The range of spacings at which propagation occurs decreases with element length. [The fire-spread rate may be nearly constant with interelement spacing over the range of spacing for which fire propagates, but in terms of fuel-bed porosity, the spread rate (and completeness of fuel burn-up) increase with voidage (and decrease with loading) over the range of voidages for which propagation occurs (Steward & Waibel 1973)]. The firebreak created by too large a separation is to be expected, but the

existence of a lower limit for element separation compatible with fire spread is less intuitively evident, since the condition occurring for small enough spacing approaches that of a continuous wooden slab, across which fire spread is quite possible. It seems that oxygen starvation (Steward & Waibel 1973) may explain the failure of flame to propagate at small enough spacings, since the spacings in question may be comparable to fuel-element thickness.

Steward et al. (1977) find that for a uniform matrix of birch dowels of fixed length, interdowel spacing, and moisture content, the fire-spread rate in still air decreases very roughly linearly with increase in dowel diameter over the range 0.25 cm to 0.64 cm. Also, for a sufficient number of columns, systematic tilt of the individual fuel elements (birch dowels), 45° from the vertical either upwind or downwind, made very little difference in the rate of fire spread in still air. Thus, it would seem that results should not be sensitive to modest random lean from the vertical of fuel elements, arising because holes are drilled in the matrix boards to hold a certain maximum number of fuel elements of a given type and because in a particular test less than that maximum number of elements are utilized in the element containing holes. Nevertheless, an effort is to be made to avoid tilting, especially in the absence of an aiding wind, since random tilting implies a nonuniform distribution.

It is perhaps cavalier to treat fuel beds generically whether they are constituted by shredded paper, needles, twigs, vertical matchsticks, wood boards arranged in a crib, or (previously unmentioned) flat parallel paper strips held on edge, such that fire propagates in the long horizontal dimension (whereas the vertical dimension of the paper strip is relatively narrow) (Emmons & Shen 1971; Prahl & T'ien 1973). For example, one hopes that the fuel-element length, voidage, and total loading for a bed of wood shavings can be related to the fuel-element length, spacing, and total loading for an array of matchsticks; i.e., one hopes that one does not have to be overly concerned with fuel-bed details to characterize flame-spread-rate variation with wind, moisture, fuel type, etc. While such simplification may seem more plausible under the circumstances of wind-aided spread of interest here, there is no guarantee of this simplicity of response. Furthermore, it should be noted that analogous parametric variations are

not always rigorously possible: the fuel loading may be held fixed while the voidage is altered in a bed of wood shavings (by arranging for a thicker distribution of shavings), but changing the voidage implies changing the fuel loading in a regular array of identical upright matchsticks. Incidentally, Steward (1974) reports that the flame-spread rate in poplar-matchstick arrays and in birch-dowel arrays was substantially faster for random (i.e., scattered to an even depth, as opposed to uniformly distributed and vertically oriented) arrangement, for tests in which the fuel type, voidage, and element length were comparable.

3.1.3 Flame Spread with the Wind.

Hwang & Xie (1984) examine the increment in fire-spread rate across vertical matchstick arrays for upslope orientation, and the decrement for downslope propagation, relative to the rate of spread for horizontal propagation. Upslope orientation induces a wind that aids spread, even if no ambient wind exists; upslope orientation also results in the flame being closer to the fuel bed to abet the radiational view-factor and contact ignition. The effect of slope seems relatively modest for orientations of no more than 10° from horizontal. Steward (1974) presents data for cribs, beds of needles, and matchsticks; the spread rate remains invariant with downslope up to 30° and more, whereas the spread rate doubles for an upslope of 20° (relative to the rate at zero slope). Cheney (1971) summarizes results of similar gist concerning the effect of slope on spread from field data gathered in Australia.

Prahl & T'ien (1973) consider wind-aided flame-spread phenomena for vertically oriented single lines of matchsticks, in the manner of Vogel & Williams (1970). However, Miller (1970) documents the need to consider sufficiently two-dimensional arrays of matchsticks in order to obtain rates of spread invariant with further increase in the number of parallel columns. Also, Prahl & T'ien engender the impressed wind via downstream suction, rather than via upwind blowing; this procedure precludes unconstrained action of the plume-type behavior, since the induction of low-level air into the plume from the downwind side is (artificially) opposed. The increment in spread rate with increasing wind (over wind-free tests) is found to level off at the higher wind speeds examined (~75 cm/s);

the authors speculate that at still higher wind speed forced-convective extinction would be anticipated.

The effect of wind and moisture content on line-fire spread across reasonably uniform beds of ponderosa-pine needles (that burned with one-meter-high flames) and white-pine needles (that burned with one-third-meter-high flames) is such that less of the fuel is burned as the wind speed increases up to 2.2 m/s (Anderson & Rothermel 1965; Rothermel & Anderson 1966). Above this speed the flaming zone was greater than the length of the fuel bed (2.4 m), and there is strong doubt that a steady rate of flame propagation was achieved; indeed, there is some doubt about whether a steady rate of propagation was achieved at an aiding wind of 1.32 m/s in the absence of published position-versus-time curves; the other cases investgated were zero wind and wind of 0.66 m/s. At the lower wind levels, moisture content below 9% is found to have but a modest effect on rate of spread. At wind of 0.66 m/s, the completeness of burn was about 45% for the 7.5-cm-thick ponderosa-pine-needles bed and was about 20% for the 5-cm-thick white-pine-needles bed; the completeness of burn doubles for each type of fuel under nil-wind conditions. The investigators, by use of a movable asbestos shield covering the downwind bed surface and of a wind-direction indicator, suggest that radiative transfer from the overhead flame is an important, perhaps dominant, mode of heat transfer to the unburned fuel elements. They also suggest that fire spreads more rapidly with increasing porosity for a fixed wind, but the supporting data are very limited.

Steward and Tennankore (1981) emphasize the longer length of run required to achieve a steady rate of flame propagation, or even a quasisteady rate, for the higher speed of spread under higher ambient wind. These investigators adopted a wind tunnel with a working section 1.22 m wide, 1.19 m high, and 7.1 m long, in which identical, vertically oriented, birch dowels arranged in a uniform matrix were burned. Center-to-center distances ranged from 0.82 cm to 3.8 cm, and the diameters of the circular-cross-section dowels ranged from 2.5 mm to 12.7 mm. "For the small diameter dowels with high rates of spread there was considerable doubt that a steady state was achieved even after 100 rows" (ibid., p. 642). The rate of fire spread was observed typically to increase by a

factor of five as the wind was increased from 0.28 m/s to 2.8 m/s for 2.5-mm-diameter dowels; but the burning time of both large-diameter and small-diameter dowels was found to be independent of wind speed for a particular fuel bed, over the range of winds just discussed. Thus, "...the width of the active burning zone is directly proportional to the rate of fire spread which...increases rapidly with wind speed" (ibid., p. 645). [Byram et al. (1966), had reported quite similar results for cribs (i.e., for fuel beds of layers of parallel pine sticks, with alternate layers parallel and perpendicular to the flow).] While the burning time of an individual birch dowel was independent of wind velocity, the burning time from 80% to 20% of initial weight was proportional to the dowel diameter to approximately the 3/2 power. Thus, whereas in a given test a 2.5-mm-diameter dowel burned in less than 20 s, a 12.7-mm-diameter dowel burned in about 200 s. "In a fuel bed with a mixture of two such diameters the 2.5 mm dowels would ignite and burn to completion before the 12.7 mm diameter dowels had virtually even started to burn" (ibid., p. 643). Such a large separation in fuel thicknesses does emphasize that flame-propagation rate is associated normally with the thin fuels present; however, in a more general context in which a more continuous spectrum of fuel sizes is present, it may be worth remarking that fire-front propagation is expected to be associated with the thinner (probably not just the thinnest) fuels present, and these more easily ignited thinner fuels, in turn, do ignite the thicker, slower-to-burn-out fuels.

Steward et al. (1977) also emphasize the difficulty of attaining steady, reproducible rates of fire propagation with an aiding wind. Especially for winds in excess of 3 m/s, spread tends to be unstable and to be dependent on the details of ignition. Nevertheless, these investigators report wind-aided-fire-spread results for birch dowels with 5% moisture content. For dowels 0.15 cm in diameter and 6.68 cm in length, the fire-spread speed is reduced to one-half if the center-to-center spacing of the array is reduced from 2.54 cm to 1.27 cm; the spread-rate increase with increase of the wind up to 2 m/s is appreciable for either spacing. (Other tests with dowels over twice as long indicated even faster spread than with shorter dowels, but these tests were cited as unstable.) However, for a wind in excess of 2 m/s, the increase of spread rate with increase of wind is much less. Indeed, at spacing of 3.81 cm, no fire

would propagate over the range of wind speeds examined (0.5 m/s to 3.5 m/s). Furthermore, for dowels of 0.64 cm in diameter, for a center-to-center spacing of 2.54 cm, the increase of rate of spread with wind is rather modest and almost independent of an increase of dowel length from 6.68 cm to 13.97 cm. Again, there is suggestion that at wind of sufficient speed, in this case 3 m/s, the increase of spread rate with wind approaches zero. In brief, a decrease of flame-spread rate with increased loading (more particularly, with decreased porosity), and a (more pronounced) increase with increased wind speed at small wind speed (but modest increase with still higher wind speed), seems to summarize the results.

Steward (1974) cautions concerning the difficulty of controlling conditions in field tests; neither the meteorological nor the fuel-bed properties are readily held constant in a test. Still, he notes that the rate of spread in pine slash, pine litter, and pine crown fires in the field increases significantly with the wind, just as the rate of spread increases significantly with the wind in the laboratory for vertically arranged white-fir sticks, poplar matchsticks, beds of white-pine needles and of ponderosa-pine needles, and beds of poplar-wood shavings--the moisture content being held fixed. With respect to the laboratory fires, Steward (1974) comments: "although... the rate of spread is substantially different from one fuelbed to another the variation of the rate of spread with wind velocity is strikingly similar." However, Steward presents no data on the completeness of fuel-bed burn-up, known to decrease with increase of wind (Fang 1969); as noted above, use of the initial fuel loading to represent the fuel consumed during flame-front passage could result in an overestimate of the heat released.

Both Thomas (1971) and Brown (1972) present data on the extent of burn up of available fuel for field experiments in the presence of an aiding wind. In fact, Thomas summarizes the results for about a dozen tests over a variety of wildlands fuels with the following expression: $v_f \sim (1 + U)/\rho_F'$, where $\rho_F' = (\sigma/L)$ in present notation. [It is recalled that L denotes the depth of the fuel bed and σ denotes the mass of fuel (per area) burned during passage of the flaming fire front.] This expression is reminiscent of (1), especially since Thomas suggests that

increase of rate of spread with wind may exceed a linear dependence for wind in excess of 4 m/s. Thomas's empirical expression is not dimensionally homogeneous and seems constructed to emphasize that a finite rate of spread occurs even for a null crosswind.

Fons (1946) systematically varied the ambient temperature, moisture content, wind, and spacing for 19-cm-long, 0.33-cm-to-1.0-cm-diameter twigs of dead ponderosa pine, set vertically and at regular intervals in fire-retardant-treated sawdust. The bed was 91 cm in width and almost 11 m in length; the upwindmost one-third of the length was set aside to permit the fire to reach an equilibrium rate of spread after line ignition of the midregion (only) of the upwindmost row. In addition to noting the reduced spread rate under lower ambient temperature (longer preheating times) and higher moisture content, Fons reported that, for the thermally thin fuel,

$$v_f \sim \frac{1}{\rho_s} \left(\frac{s}{d}\right) U^n \ , \qquad (6)$$

where $n \doteq 1$ for winds under 2.25 m/s and $n \doteq 1.5$ for winds between 2.25 m/s and 9 m/s. This is somewhat of the character $v_f \sim U^n/\sigma$; Fons noted that spread must slow and desist for sufficiently large spacing s.

While some general trends are evident, definitive insight is not available yet in the literature.

2.4 EXPERIMENTAL TESTS.

2.4.1 Test Facility.

The facility used in the present investigation has been described in detail previously (Fleeter et al. 1984), but brief comments are included here so that the presentation is selfcontained.

The facility consists of a blower which pushes ambient air through a flow-conditioning section upwind of the test section (Figure 1). Through the use of a sequence of honeycombs, fine screens, and felt filters, all at least several meters upwind of the test section, the flow preparation section produces a uniform steady stream of low turbulence. Specifically, the streamwise speed varies by less than ±5% from the mean wind velocity (Figure 2), and the pertinent Reynolds stresses were determined to be less

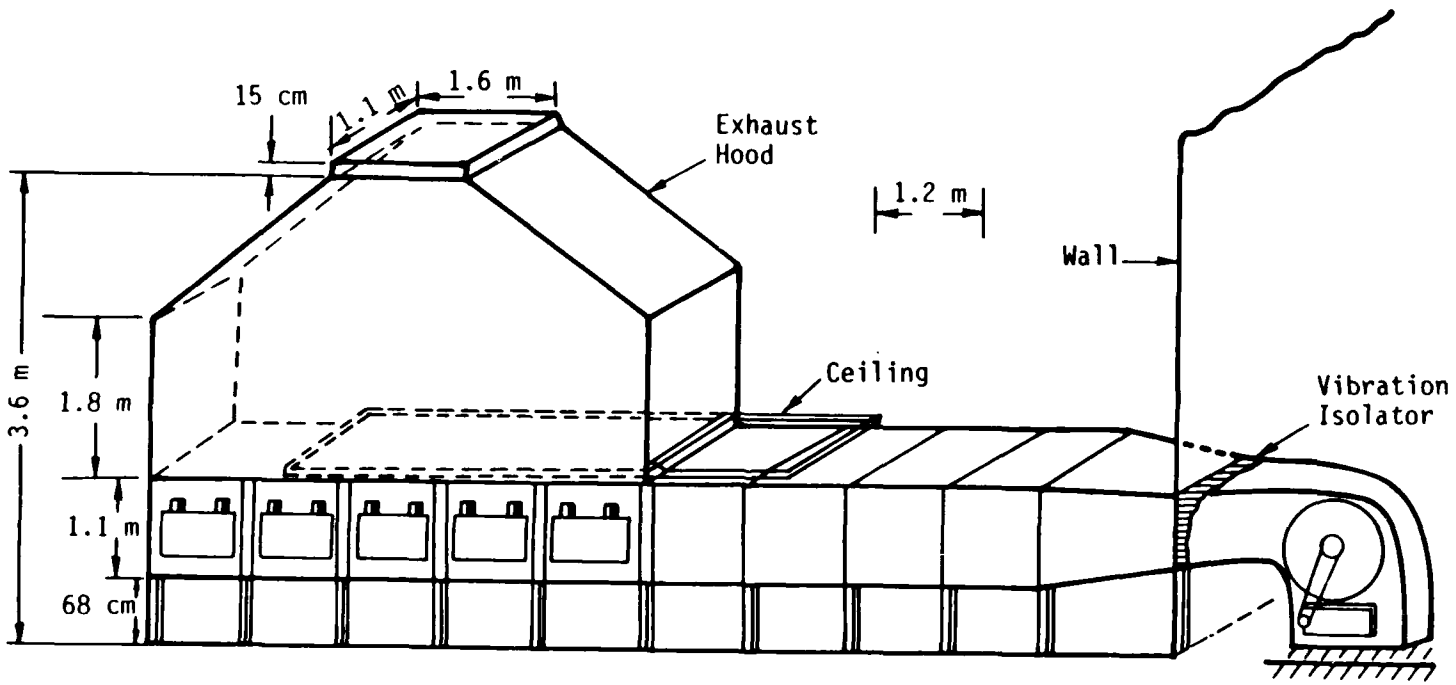

Figure 1. Fire-tunnel facility for wind-aided-spread experiments: external blower, flow preparation section, side-view windows and movable ceiling for the test section, and tall exhaust hood.

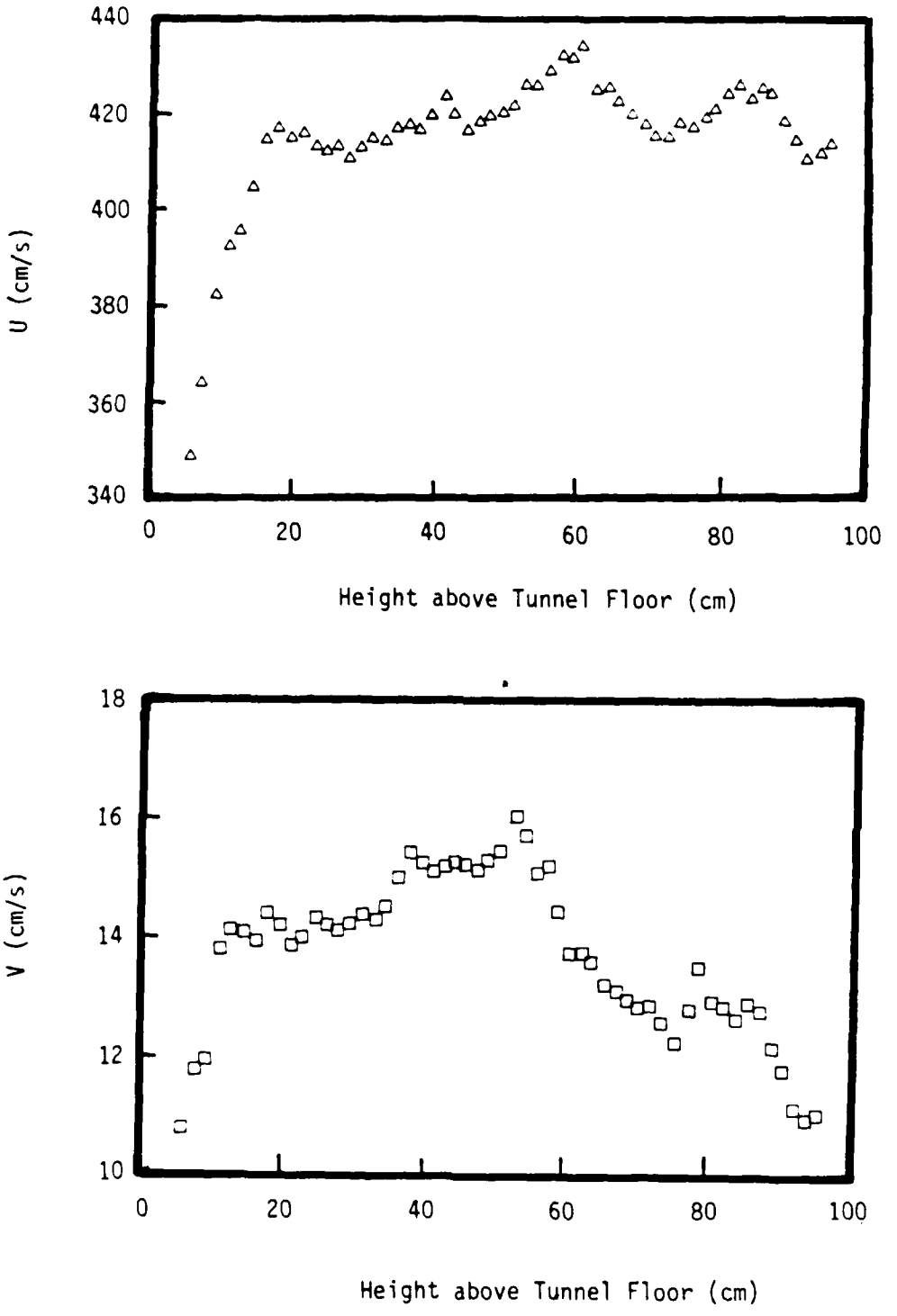

Figure 2. Hot-wire measurements along the centerline of a vertical cross section at the beginning of the test section, for a nominal streamwise velocity component U of 4.2 m/s. The vertical velocity component is denoted V.

than 5 cm^2/s^2 [Figure 3, wherein U denotes (time-average) streamwise speed, V denotes (time-average) transverse speed, prime denotes fluctuation from the mean, and super bar explicitly denotes time average). The wind tunnel has a movable ceiling, readily capable of translation downwind in its own plane, such that the leading edge of the ceiling can be made to trail just behind the downwind-propagating buoyant flaming upflux. The fire plume is concentrated in the vicinity of a narrow burning front that separates uninvolved downwind fuel from whatever char remains of the fully outgassed upwind fuel.) Provision for the movable ceiling permits the buoyant plume to rise with a minimum of obstruction, while also allowing an airflow of undiminished freestream speed to reach the propagating fire front, since the upwind cross-sectional area is maintained constant during the fire spread. (Of course, the thickness of the near-fuel-bed boundary layer does increase with downwind distance from the leading edge of the test section, but the dimensions of the cross section, over 1.1 m x 1.1 m, assure that no appreciable acceleration of the freestreaming occurs.) Aiding winds in excess of 4 m/s are attainable in the tunnel.

The 5-m-long fuel bed consists of ceramic trays with holes drilled at 1-cm intervals; i.e., the fuel bed may be envisioned as a checkerboard with a hole drilled at the center of each square, of 1-cm-edge dimension. The discrete fuel elements utilized here are thin white-pine toothpicks, oriented vertically, with 0-to-4 toothpicks per hole (Figure 4). The test-initiating ignition involves simultaneously lighting all the fuel elements in the upwindmost line (row), perpendicular to the airflow. The air and the rising plume exit without obstruction through an exhaust stack into the atmosphere.

The rate of fire-front propagation is indicated by type-K thermocouples, spaced at 14-cm intervals along the centerline of the test bed in the direction of the air flow. The readings are recorded digitally on a MINC PDP 11/23 computer. Since only time of pyrolysis-temperature onset is used to indicate fire-front transit, any delay in relaxation to ambient temperature is of no concern for current purposes. No reference junction is provided since the temperature range of interest far exceeds ambient levels (373 K to 1373 K). The thermocouple voltages are converted to temperatures and are presented as functions of time. In addition, a

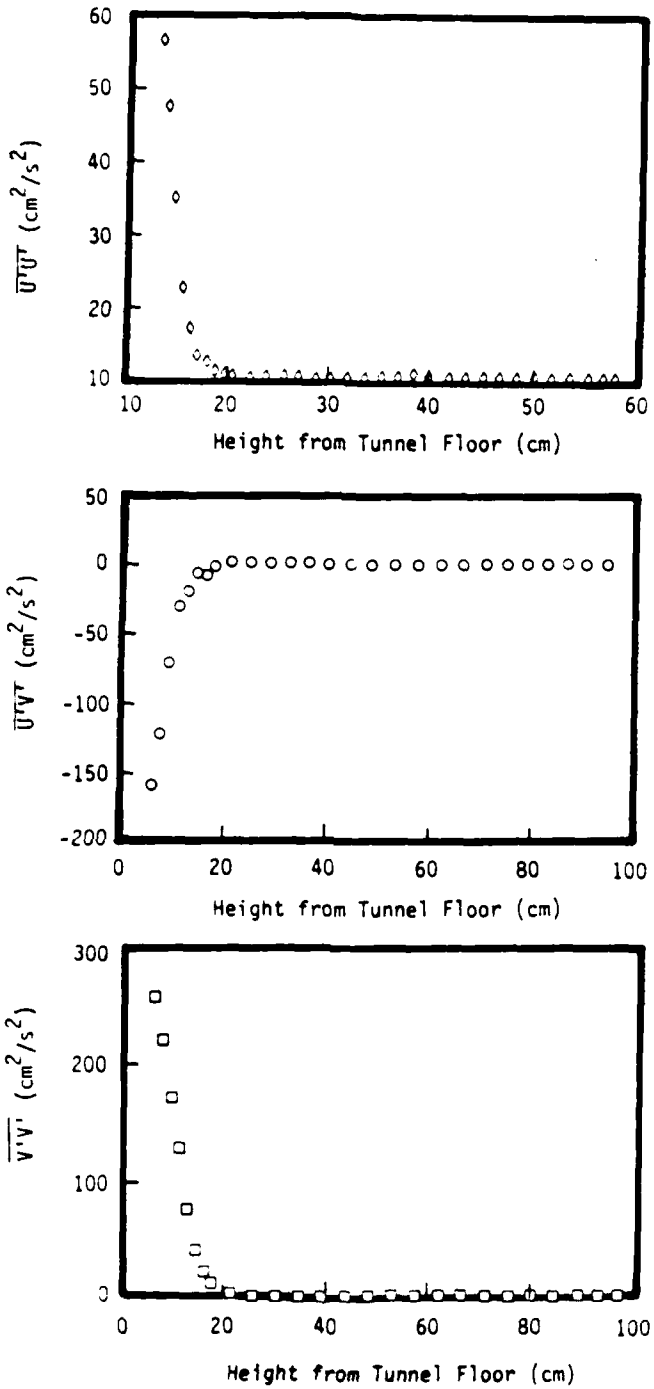

Figure 3. Density-normalized Reynolds stresses along the centerline of a vertical cross section at the beginning of the test section, for a nominal streamwise velocity component U of 4.2 m/s. Vertical velocity is denoted by V; fluctuation from the mean, by a prime; time average, by a super bar.

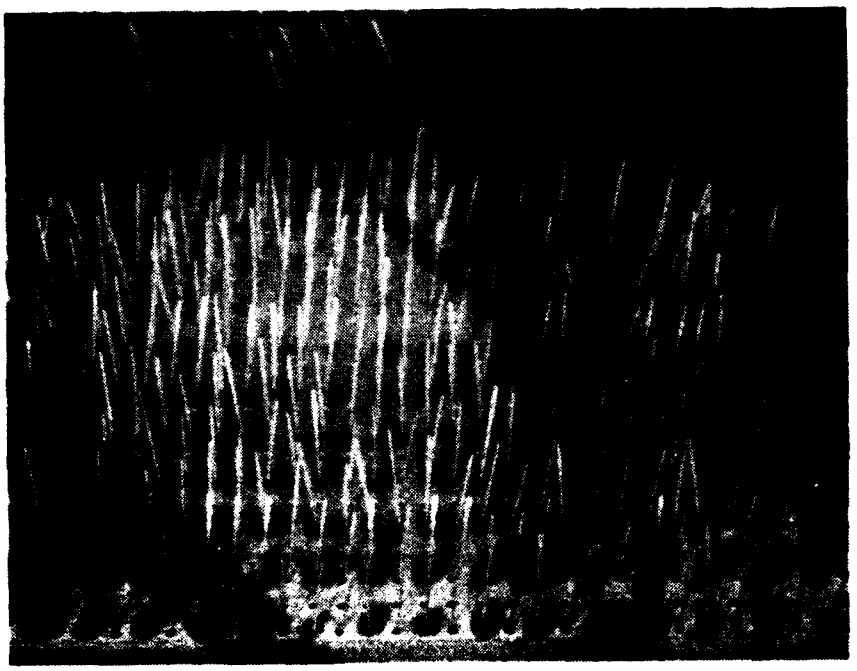

Figure 4. Ceramic trays, drilled with holes one centimeter apart, filled with a toothpick loading such that $\sigma = 0.02208$ g/cm^2.

side-view record of a test is obtained by manually moving a video camera mounted on a translatable platform outside the tunnel. An overhead view of a test is obtained by use of a video camera attached to the ceiling.

2.4.2 Test Conditions, Data Analysis, and Repeatability.

Attention was concentrated on the ascertaining the dependence of flame-propagation rate on three parameters anticipated to be of particular importance (Table 1): the wind speed (varied from 0.7 m/s to 4.1 m/s); the average fuel loading (varied from 0.011 g/cm^2 to 0.088 g/cm^2); and fuel-bed width (varied from 30 cm to 100 cm). Other parameters, such as fuel-element height, fuel-element thickness, fuel-element composition, and fuel-bed inclination relative to horizontal, were held constant. Ambient temperature varied from 273 K to 289 K, and the ambient relative humidity varied from 15% to 75%; however, the flame propagation rate was judged to be insensitive to these variations.[4]

The individual flat-sided white-pine toothpicks used were 6.1 cm in length, with about 4.8 cm exposed for burning above the drilled ceramic tray. The circumference of the lengthwise-varying-rectangular-cross-section toothpicks was such that the average equivalent diameter for a circle was 0.17 cm, and the average mass per toothpick was about 0.052 g. Toothpicks, even in the tests with the widest loading distributions (100 cm), were more than 5 cm from the tunnel-test-section side walls.

A typical thermocouple-output curve of temperature as a function of time describes a slow rise in temperature (interpreted as preheating), followed by a more rapid rise (interpreted as flame arrival), followed by a gradual decay (interpreted as forced-convective cooling of the thermocouple by the upwind air flow). In the convention adopted here, the flame front

---

[4]Approximately 500 toothpicks at a time were subjected to the gross-heat-of-combustion technique specified in the National Fire Protection Association protocol 259 (Standard Test Method for Potential Heat of Building Materials); the tests were conducted in an isothermal jacketed oxygen bomb calorimeter. The test sample was stored in a conditioning room (held at 296 K ±3 K, 50% ±5% relative humidity) for about two months. Each sample was then ground via a rotary laboratory mill until it would pass through a 60-mesh screen, then returned to the conditioning room for a week before testing. The gross heat of combustion was about 17.7 kJ/g of fuel. (Continued)

Table 1. Fire-Tunnel Data.

Wind Speed U (cm/s)	Fuel Loading σ (g/cm^2)	Bed Width W (cm)	Flame Speed v_f (cm/s)	Error Bar[a] v_f (cm/s)
0[b]	0.04415	55	0.0	0.0
68[c]	0.08830	55	0.9	0.8-1.0
68[d]	0.04415	55	1.3	1.0-1.5
68	0.01104	55	1.8	1.7-1.9
90	0.04415	55	1.6	1.5-1.7
137	0.03200	55	3.2	2.9-3.2
145	0.04415	55	2.2	1.9-2.5
200	0.08830	55	1.3	1.3-1.7
200	0.04415	30	1.8	1.8-1.9
200	0.04415	55	2.8	2.1-3.4
200	0.04415	55	2.2	1.9-2.3
200	0.02208	30	2.7	2.3-2.9
200	0.02208	55	4.4	4.2-5.6
200	0.02208	55	3.3	3.3-3.6
200	0.02208	55	4.0	3.8-4.8
200	0.02208	55	4.3	4.2-4.8
200	0.02208	55	4.2	4.1-5.3
200	0.02208	100	7.3	7.0-7.6
200	0.02208	100	8.5	7.8-9.3
200	0.02208	100	6.5	6.1-7.8
200	0.01104	30	3.7	3.6-4.2
200[e]	0.01104	55	4.0	3.7-4.3
200	0.01104	100	6.8	6.2-7.4
310[e]	0.08830	55	1.0	0.9-1.4
310	0.04415	55	2.7	2.6-4.7
310	0.02208	55	4.9	3.5-5.2
310[e]	0.01104	55	4.2	3.8-4.9

Table 1. Fire-Tunnel Data (Continued).

Wind Speed U (cm/s)	Fuel Loading σ (g/cm^2)	Bed Width W (cm)	Flame Speed v_f (cm/s)	Error Bar[a] v_f (cm/s)
350[e]	0.04415	55	1.8	1.8-2.8
415	0.04415	55	2.8	2.1-3.4
415	0.01104	56	6.4	5.0-6.5

[a] The error bar is based on a subjective estimate of the span of "reasonable" slopes assignable to the thermocouple data of flame-front position as a function of time.

[b] Two trails with different crystallinity are summarized.

[c] Four trials with different crystallinity are summarized.

[d] Nine trials with different crystallinity are summarized.

[e] This case seems at odds with general trends (explicitly, the speed of fire propagation seems slow); this case is to be repeated during further testing. In general, the error bar increases for cases entailing larger flame speed v_f, i.e., cases in which U, W, and σ^{-1} tend to be larger.

is taken to have reached a specific thermocouple when the temperature first exceeds 673 K. Since the rise in temperature is very rapid as the flame front passes over the thermocouple (Figure 5), adoption of 573 K or 773 K as the criterion for fire-front arrival would have minor consequence on the position of the fire front in time, as reported on the basis of 673 K (Figure 6). A constant rate of flame propagation, i.e., for a steady spread, is evidenced by the curve in Figure 6 approaching a straight line; for minor deviations from strict linearity, a least-squares fit of the data to a linear function (with any transient interval discarded) yields the fire-propagation rate.

Several tests were conducted under nominally the same conditions on different days to investigate the repeatability of results. The case in question entailed a wind speed of 2 m/s, a fuel loading of 0.022 g/cm^2, and a test-bed width of 55 cm/s. The humidity varied by 20%, and the ambient temperature varied by 4 K, between the tests. Scatter owing to uncontrolled variables seemed to be minimal.

2.4.3 Spread Rate as a Function of Crystallinity.

It has already been noted that, if effectively identical toothpicks are inserted upright into the drilled holes, fuel loading is altered only by varying the porosity. The porosity is varied by the number of toothpicks and/or the spacing between toothpicks. Attention is confined to regular arrangements, such that only small-scale inhomogeneity within a fuel bed uniform on a grosser scale is permitted ("crystallinity"). In particular, the allotment of toothpicks to the smallest four-hole square delineated by drilled holes constitutes the basic fuel-loading "building block"; this element is meticulously repeated to comprise the entire array for the tests reported here.[5]

---

[4] (Continued) Samples were also placed in an oven at 373 K for 48 hours prior to testing to remove free water (which proved to constitute 7% to 8% by mass of the sample). The gross heat of combustion then was about 19.0 kJ/g. The authors are very grateful to J. R. Lawson of the Center of Fire Research of the National Bureau of Standards for this data. Independently, after typical storage, baking 100 toothpicks at 573 K for 16 minutes removed 8.4% of the toothpick mass.

[5]For a square grid of holes, each of which can accommodate up to and including four toothpicks, for a four-hole-square basis there are four ways to achieve the equivalent of one-half a toothpick per hole, eight ways to

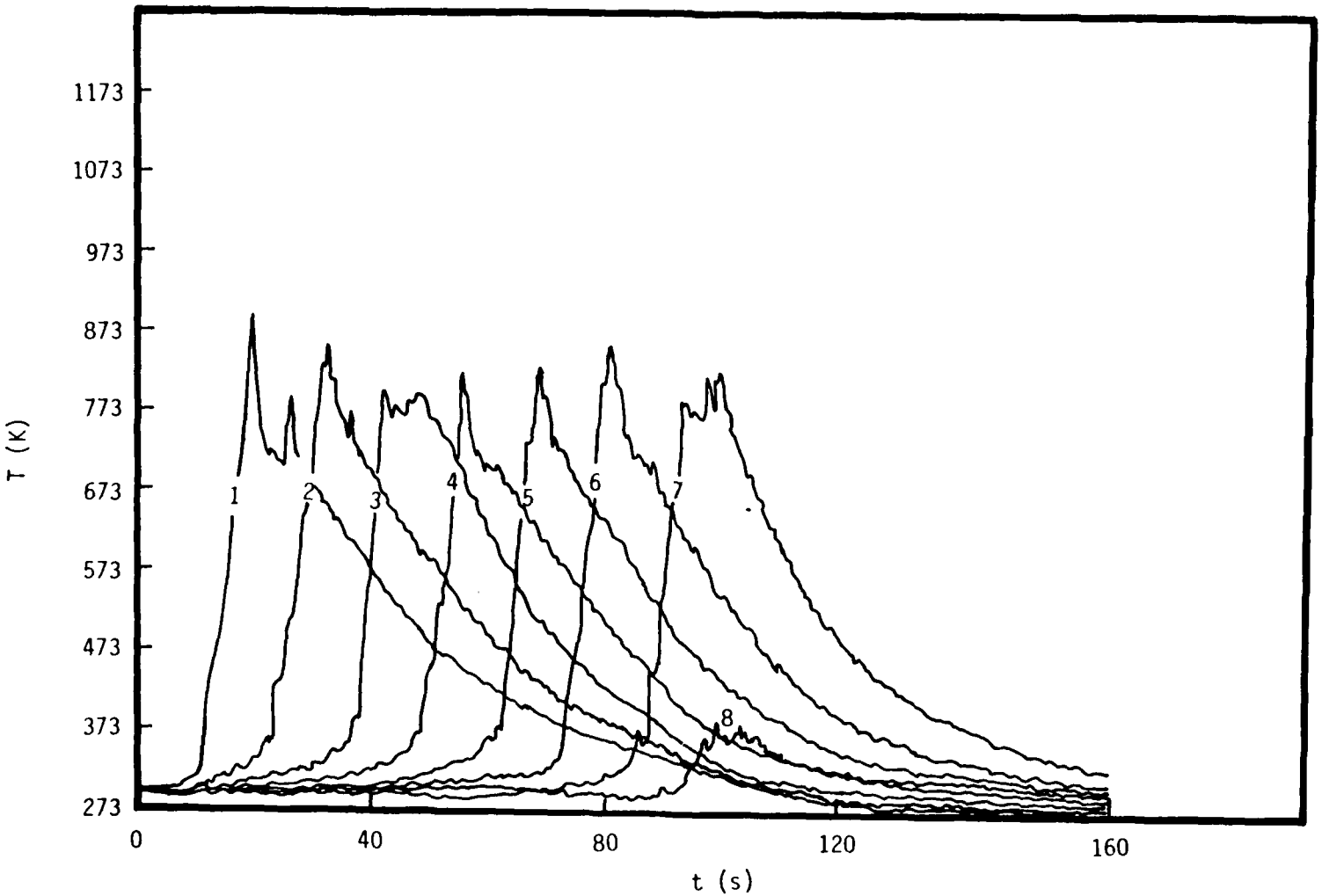

Figure 5. From typical centerline-thermocouple traces, the temperature T is presented as a function of time t since ignition; successive thermocouples are 14 cm apart.

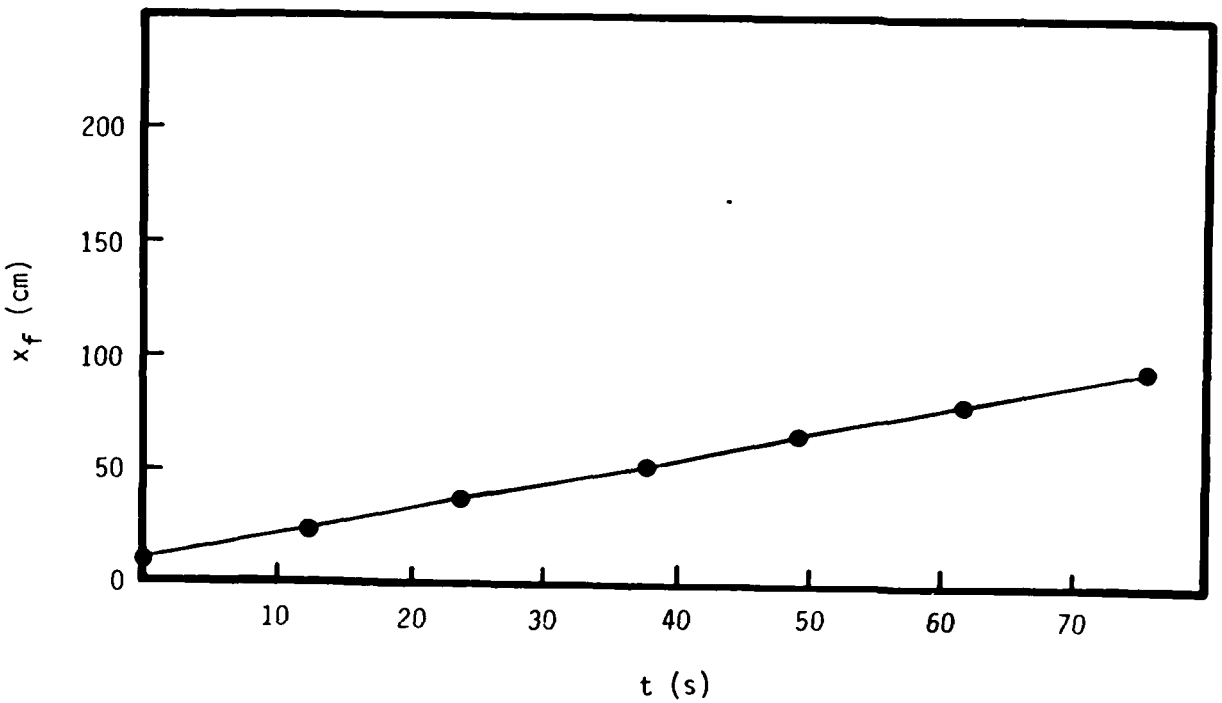

Figure 6. For the data of Figure 5, with 673 K taken as the temperature at the time of flame-front passage, the fire-front position (distance downwind of the leading edge of the fuel bed) x_f is presented as a function of time t since ignition.

Thus, one can obtain an average of one toothpick in each hole by placing a single toothpick in every hole or by placing two toothpicks in every other hole.

Figure 7 indicates the sensitivity of fire-spread rate to details of fuel-element distributions in which there is the equivalent of two toothpicks in each hole; Figure 8 indicates the sensitivity for variations on the equivalent of one toothpick per hole.[6] Results indicate that the fire-propagation rate is somewhat sensitive to details of the fuel loading for the lighter loadings investigated.

2.4.4 Spread Rate as a Function of Wind Speed.

Wind speed U was varied from 0.8 m/s to 4.1 m/s in the tests conducted. (Flame did not propagate in the absence of wind for any arrangement of any loading examined.) An increase in the wind speed generally resulted in an increase in the flame-propagation speed v_f, with the dependence approximately being directly proportional to the square root of the wind (Figure 9). However, the rate of spread appeared to reach a plateau at larger wind speeds, especially for heavier loadings, the asymptotic value being dependent on fuel-bed loading and width. This asymptote appears to be an aspect of the physical phenomenon of interest, but additional runs are required to rule out attribution of the behavior to artifacts associated with the facility.

---

[5] (Continued) achieve the equivalent of one toothpick per hole, and sixteen ways to achieve two per hole--if one precludes subdividing toothpicks and disregards effectively equivalent arrangements. It is conjectured that the flame will propagate faster for those arrangements, with fixed wind speed and fixed fuel loading, for which a downwind element is closer to an upwind element, with both oblique and in-line considerations of consequence. However, it is anticipated that details of small-scale nonuniformity is not of great import on spread rate.

[6] Presence of more than one toothpick per hole augments the possibility of shading of one fuel element from some radiation owing to another. Incidentally, virtually all synthetic polymers available in toothpick-type configuration are thermoplastics, which melt upon heating. Such a pool of fluid combustible is not suitable for the finite-thickness-front fire propagation sought for steady spread. Thus, attention is limited to natural polymers.

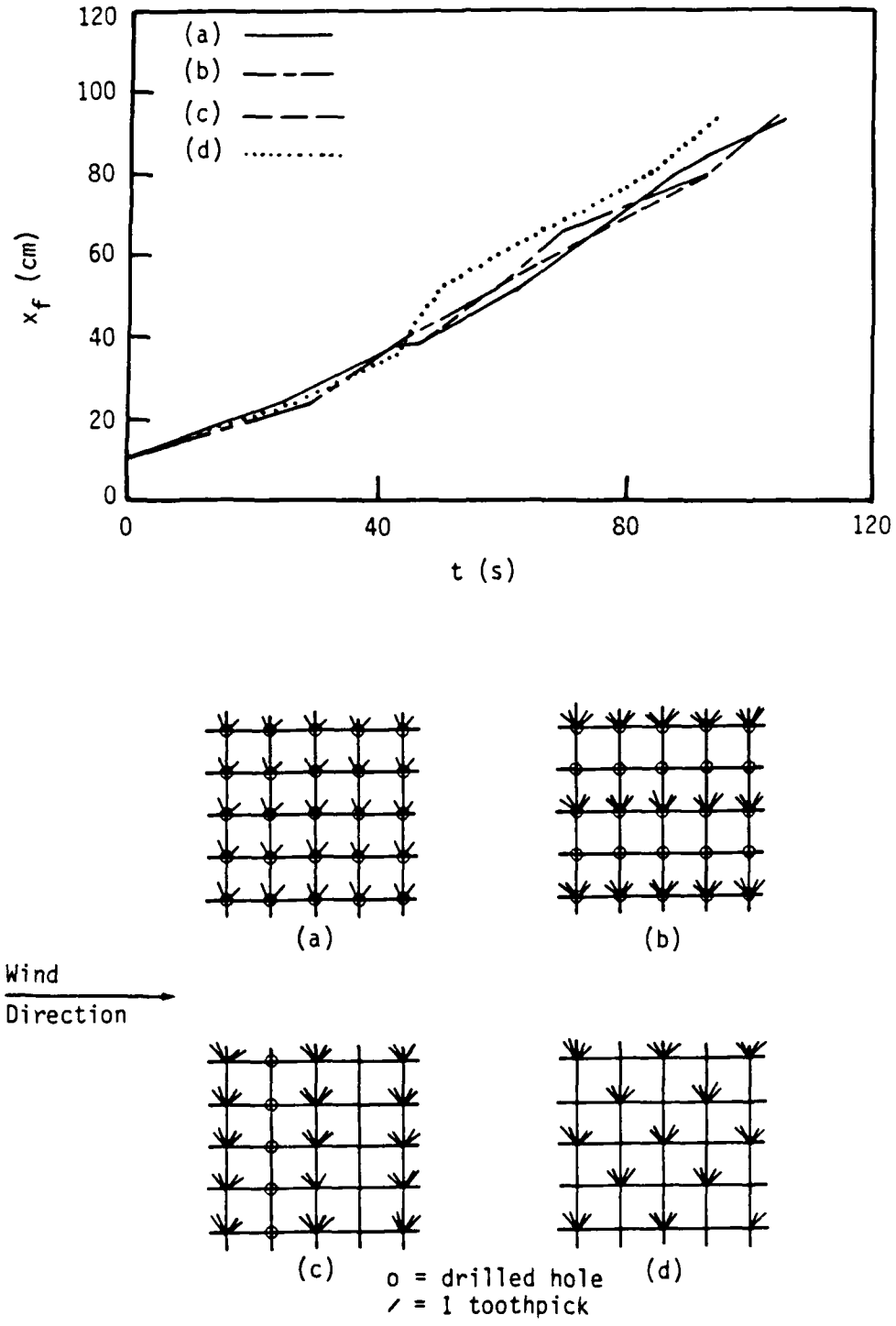

Figure 7. Effect of the loading pattern on flame-front propagation at fuel loading σ = 0.08830 g/cm^2, bed width W = 55 cm, and wind speed U = 70 cm/s. The quantity x_f is the flame-front position and t is time since ignition.

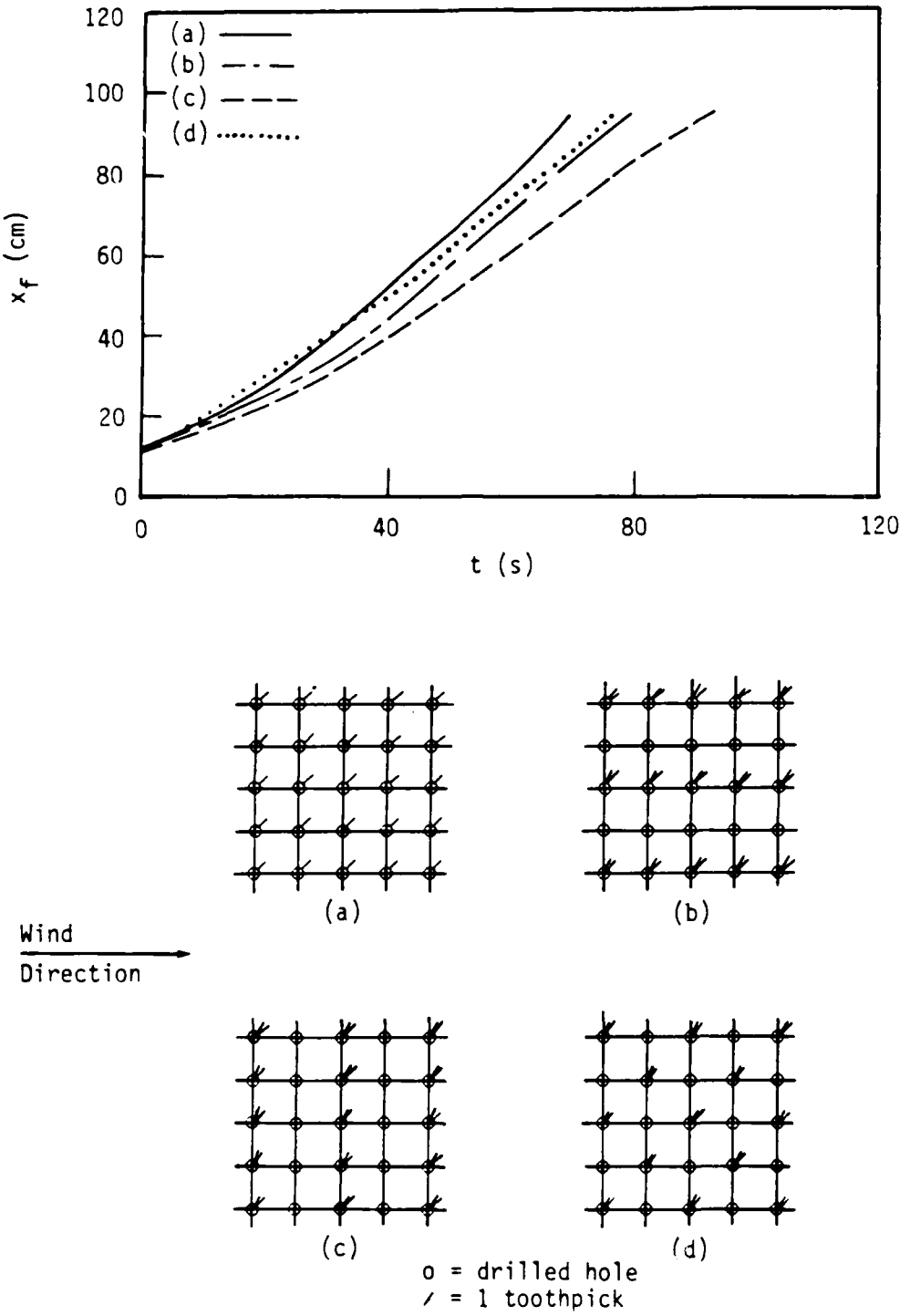

Figure 8. Effect of the loading pattern on flame-front propagation at fuel loading σ = 0.04415 g/cm^2, bed width W = 55 cm, and wind speed U = 70 cm/s. The quantiy x_f is the flame-front position and t is time since ignition.

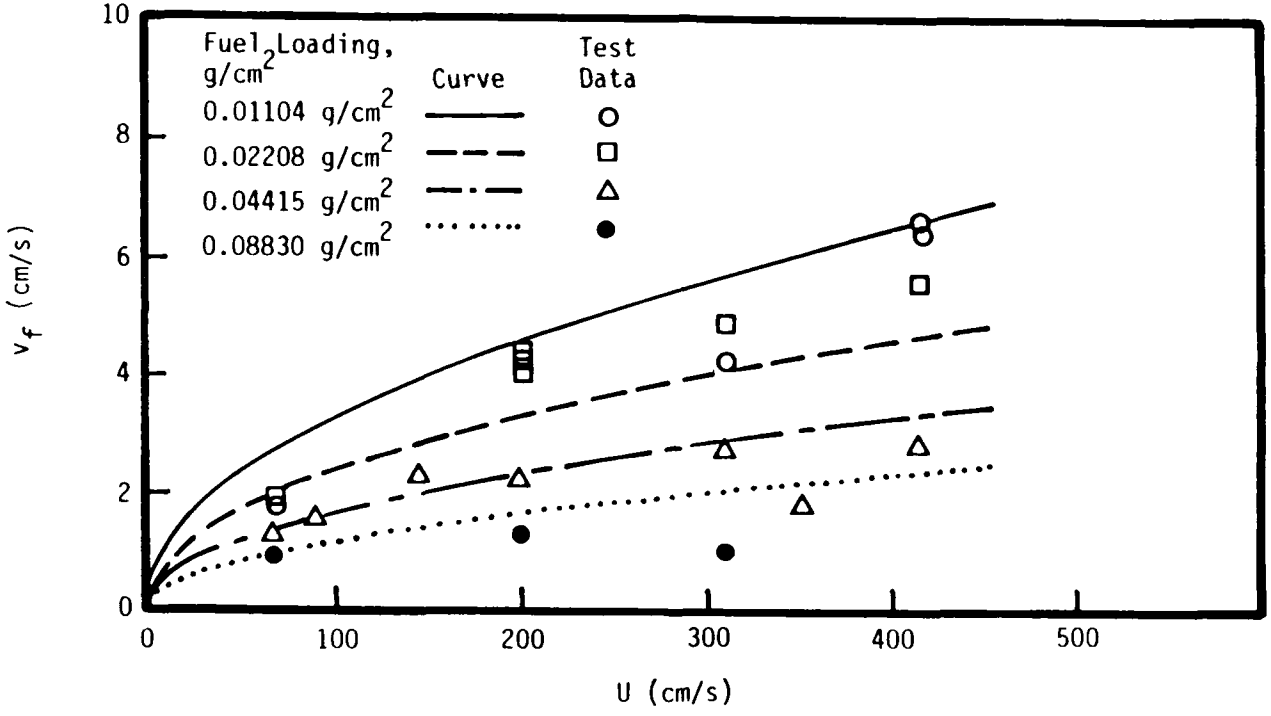

Figure 9. Flame speed v_f as a function of wind speed U, for bed width W = 55 cm. A curve fit to the data is given by $v_f = 0.034\ (U/\sigma)^{1/2}$, with v_f in cm/s, U in cm/s, and σ in g/cm^2.

2.4.5 Spread Rate as a Function of Average Fuel Loading.

Figure 10 indicates that the flame speed v_f generally increased as the fuel loading, σ was decreased from 0.088 g/cm^2 to 0.011 g/cm^2, with the dependence approximately being inversely proportional to the square root of the loading. However, for too small a density of fuel, fire would not propagate along the discrete fuel array: too great a spacing between adjacent elements created a firebreak. Variability of rate of spread between nominally identical cases increased with decreased loading.

2.4.6 Spread Rate as a Function of Fuel-bed Width.

The flame speed v_f increases linearly and directly with the width W of the fuel bed, as the fuel-array width was varied from 30 cm to 100 cm (Figure 11). The increase in flame speed with the increase in the test-section width is ascribed to downwind fuel elements receiving radiative heating from a wider burning area. It may be noted that the fire front propagates more rapidly near the centerline of the fuel array than along the lateral edges (Figure 12). This behavior seems attributable to the fact that a downwind near-centerline fuel element receives radiative heating from both sides, while an edge fuel element is irradiated from only a single side.

2.5 CONCLUSIONS AND RECOMMENDATIONS.

Wind-aided fire propagation across two-dimensional horizontal matchstick-type arrays were measured in a specially designed wind tunnel. Results to date indicate that the flame-propagation speed v_f is related to the wind speed U, the fuel loading σ, and the fuel-bed width W by

$$v_f \sim W\,(U/\sigma)^{1/2}, \qquad (7)$$

over the parameter domain investigated. The flame-front curvature, fire-plume tilt, and flaming-front thickness also depends on these parameters.

Futher investigation is intended to obtain more definitive and comprehensive results for the parametric domain already scanned, and to consider the effect on flame speed of other parameters such as fuel-element

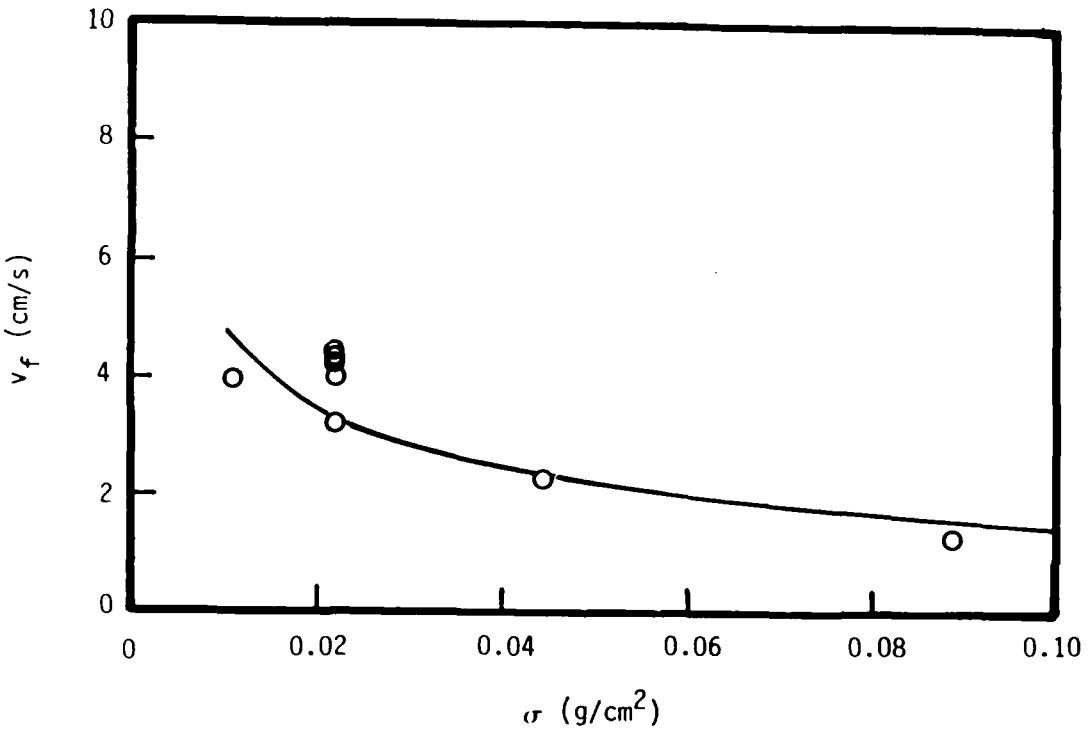

Figure 10. Flame speed v_f as a function of fuel loading σ at wind speed U = 200 cm/s and bed width W = 55 cm. The curve is given by $v_f = 0.034\ (U/\sigma)^{1/2}$.

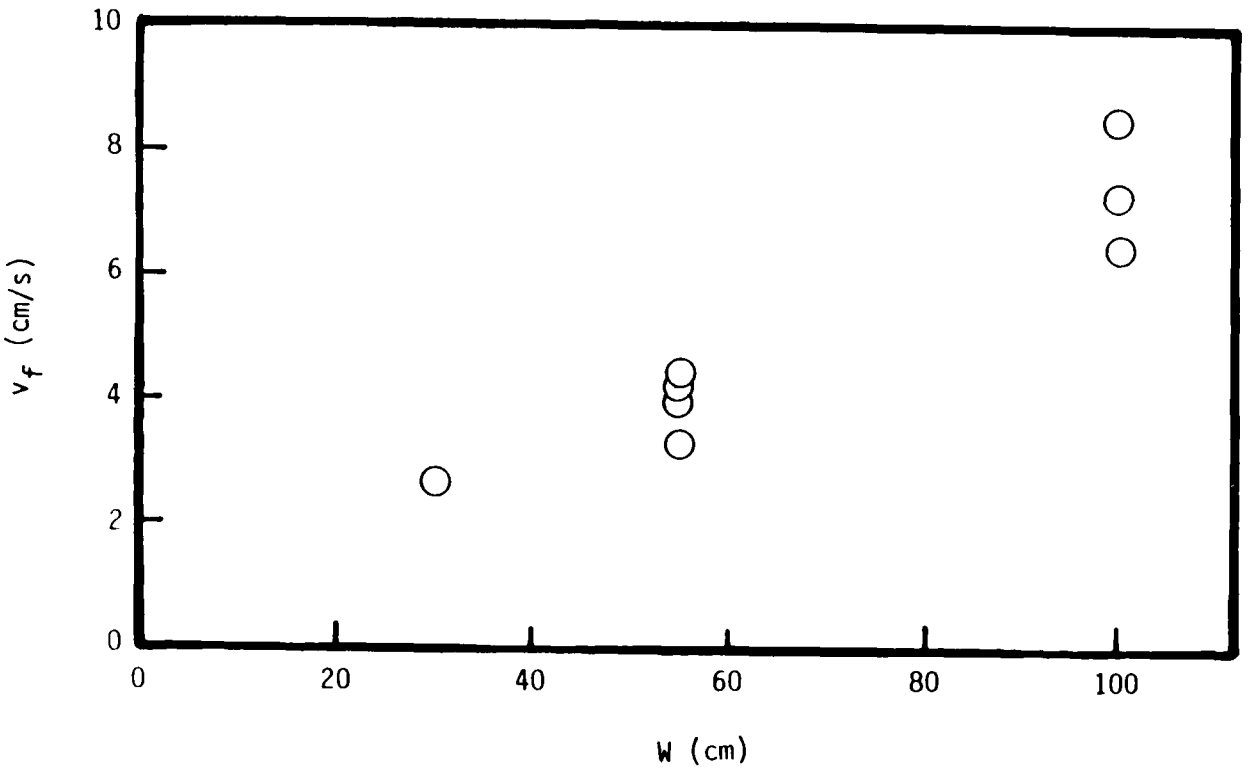

Figure 11. Flame speed v_f as a function of test-section width W at wind speed U = 200 cm/s and fuel loading σ = 0.02208 g/cm^2.

Figure 12. Curvature of the downwind-tilted (leftward-propagating) flame front, enveloping burned-out fuel (wind speed U = 2 m/s, bed width W = 1 m, fuel loading σ = 0.01104 g/cm^2).

height, fuel-moisture content, fuel-bed tilt, and presence of noncombustible heat-sink-type material ("rubble").

The intention is to add several tandem calorimeters on the centerline in the downwind fuel bed to infer the temperature of the flaming front irradiating the still-uninvolved fuel elements. Another planned addition is a vertical array on the centerline of thermocouples (or velocity sensors) to indicate the thickness of the near-bed boundary layer as a function of distance upwind of the fire front.

More specifically, in principle a semi-empirical modeling might proceed thus. A coordinate system is adopted that translates laterally at the (by postulation, constant) fire-front-propagation speed, and vertically at the negative of the local speed associated with the interphase mass transfer (from solid to gas). In this coordinate system, a steady treatment (in the parabolic approximation) of the so-called Emmons problem seems applicable to the upwind fire-front. This problem concerns the description of a thin gas-phase diffusion flame over a pyrolyzing solid fuel. The base of the buoyant flaming front would lie at the downwind position at which the fuel bed is effectively fully outgassed. The vertical tmperature profile at this flaming front implies the radiative transfer that preheats the downwind fuel from its ambient temperature to its pyrolysis temperature at the flame-front position. The empiricism enters in the treatment of turbulent transport and fire-front thermal nonuniformity.

SECTION 3

WET-COAGULATION-OF-SMOKE EXPERIMENT

3.1 OBJECTIVES.

The main objective of the laboratory experiment is to ascertain whether wet coagulation can be an important process for smoke in a cloud.[7] Wet coagulation is only one of several processes that befalls smoke particles enveloped in a cloud (Twomey 1977; Slinn 1984; Goldberg 1985). Referring to Figure 13, we see that the possibilities include (but are not necessarily limited) to the following.

- Smoke particles become cloud condensation nuclei (CCN) and cloud droplets are formed around them. There is some evidence that this may happen to only 5% of the fresh smoke particles. (After aging, another 10% may become CCN). The reason is that smoke particles, primarily soot, are carbon-spheroid aggregates. They are not soluble and wettable. However, with aging, surface deposition on (agglomerates of) the particles may alter these properties.
- Smoke particles may be "scavenged", i.e., collected by cloud droplets and subsequently deposited with rain. Results of the White Face Mountain Experiments (reported by Rudy Pueschel of the NASA Ames Research Center at the DNA Global Effects Program Meeting, Moffett Field, Ca, 25-27 February 1986) indicate that as much as 97% of the smoke may have been removed by this process.
- Wet coagulation is related to scavenging. Smoke particles first are collected by cloud droplets, which may evaporate when they leave the cloud; a soot agglomeration remains. These larger soot particles have higher sedimentation velocity. Even if they remain aloft, because of their larger size, they would be less efficient with respect to the extinction of sunlight (see Figure 14).

---

[7] If it is demonstrated that a careful simulation of capping-cloud phenomena almost invariably results in either a highly significant or a highly insignificant effect on a smoke aerosol, then the experiment furnished informative guidance. If the significance of the effect is highly conditional, then the adequacy of the simulation requires close scrutiny.

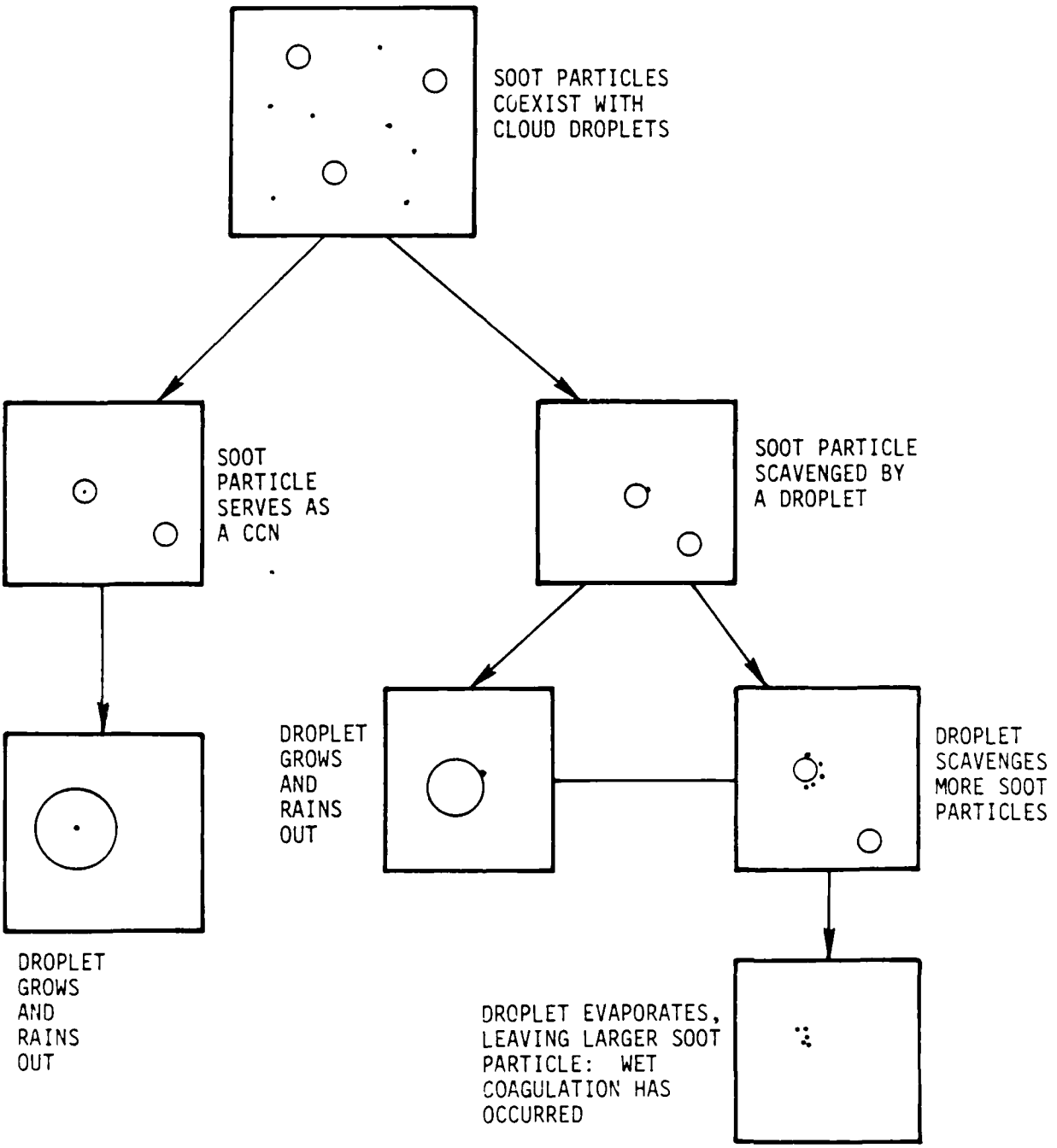

Figure 13. Some possible paths for the interaction of soot particles with cloud droplets.

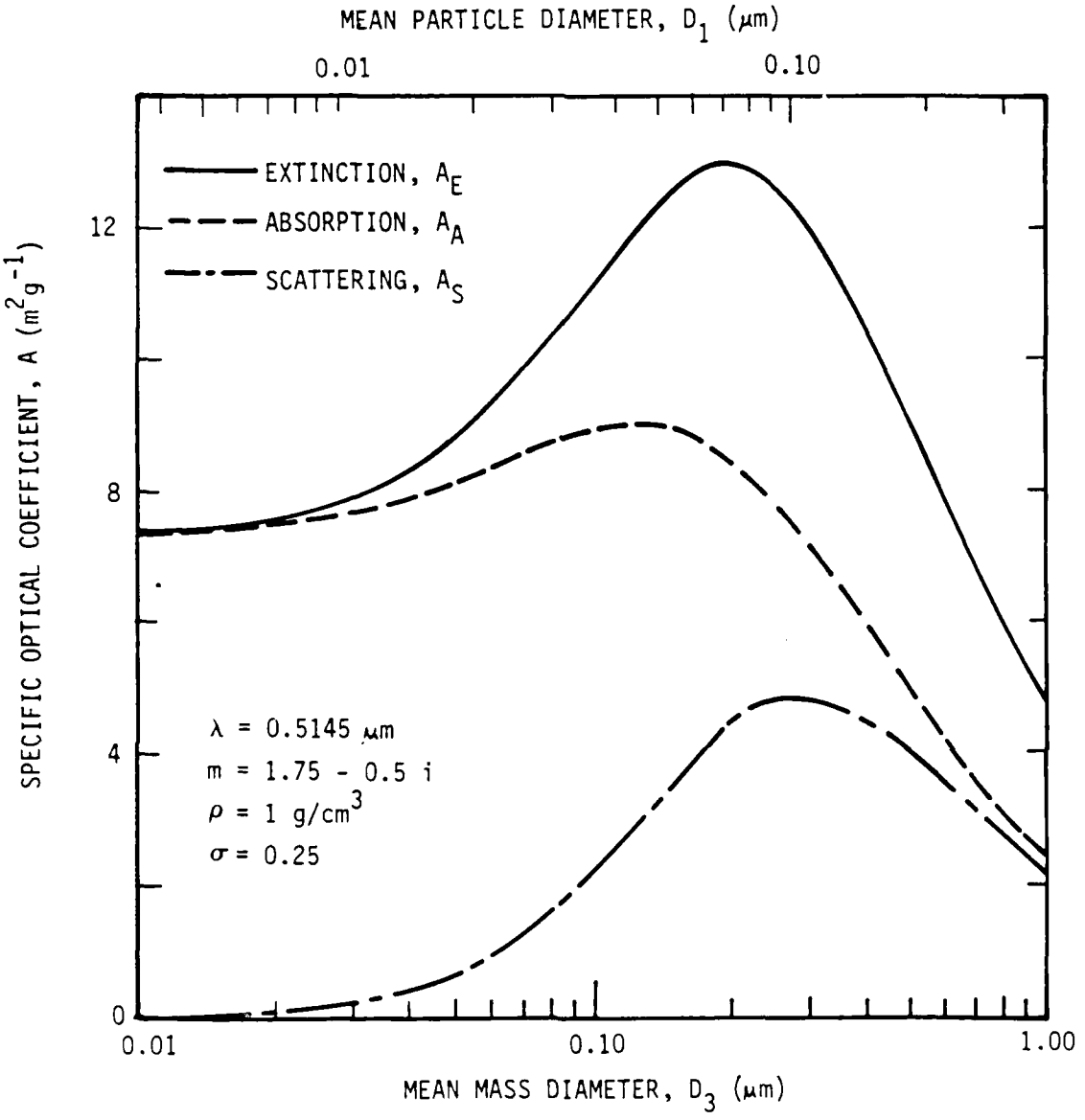

Figure 14. Theoretical variation of the specific absorption, scattering, and total extinction coefficients of spheres of density ρ = 1 g/cm^3 and refractive index m = 1.75 - 0.5 i at wavelength λ = 0.5145 μm as a function of mean particle size. The geometric mean standard deviation σ is defined by $\sigma^2 = [\log_{10}(D_3/D_1]/6.91$. (From Roessler and Faxvog 1979).

To study wet coagulation, we need to maintain coexistent smoke and cloud droplets in a cloud chamber for a period of time. We also need to make the following measurements before and after the test interval:

- o size distribution of the soot particles, and
- o coefficient of extinction of light by the soot particles.

These two measurements are related but not redundant. If we measure only the size distribution before and after the test interval, we may find that there is a change in size, but we would not be sure that the extinction coefficient has changed. This ambiguity arises because the soot particles are chain aggregates (rather than spheres), with some consequent uncertainty in the index of refraction. Theoretical estimates of the extinction on the basis of size alone would be only approximate. Alternatively, if we measure only extinction and find that there is a change in transmitted light, we would not be sure if it were due entirely to increase in size because of wet coagulation, or partly to decrease in number density because of scavenging and rain out. If extinction is measured with proper accounting for particle losses to the wall and to rain out, then hopefully both measurements would be consistent.

Two other processes related to soot interaction with cloud droplets, namely, soot particles acting as CCN and scavenging of soot by cloud droplets, also can be investigated with our experimental setup.

3.2 EXPERIMENTAL DESIGN.

In this experiment, we are trying to simulate what may happen in a natural process: smoke, rising with moist air, cools adiabatically as it ascends to (say) 10 km, near which height it may be supposed that a cloud is formed. The experimental design obviously has to consider the following questions.

- o How are adiabatic expansion and cloud-chamber cooling to be carried out?
- o How is a cloud to be sustained? What number density and what size should characterize the droplets?

In addition, of course, we need to consider the following matters.

- o How is the size distribution of the soot particles to be measured?
- o How is the optical extinction by the smoke to be measured?

We now consider each question sequentially.

3.2.1 How Are Adiabatic Expansion and Cloud-Chamber Cooling to Be Carried Out?

There are three ways to achieve adiabatic expansion: evacuation, expansion by pulling a diaphragm, and expansion by pulling a piston. Evacuation is the method used, for example, for the cloud chamber at the University of Missouri at Rolla. Digital valves are used to control finely the rate of evacuation. We decided against using this approach because some of the particles and moisture will be lost in the process of evacuation and recompression: after the smoke has been confined with the cloud for a specified time, we need to recompress in order to evaporate the cloud for the light-extinction measurement. Evacuation, therefore, seems not to meet our requirements.

We can circumvent the above objections by using a chamber with a diaphragm in the middle. By pumping on one side, gas on the other side of the diaphragm may expand, hopefully adiabatically; compression can be accomplished by reversing the process. However, the diaphragm would not be cooled actively and would be a heat source to the gas, with considerable extraneous convection resulting. For this reason, we also reject the diaphragm method.

The piston-expansion method traditionally has been used in a quick-expansion cloud chamber. It is more costly because the chamber has to be bored straight. There is concern regarding possible leakage of mass around the piston ring as the chamber is taken to low temperature. This can be minimized by choosing a closely fitting ring seal and by pumping on the other side of the piston to equalize the pressure. Despite the reservation, we choose the piston method because the piston can be actively cooled.

At two of the major cloud-chamber facilities with wall-temperature control in the United States, of the University of Missouri at Rolla (UMR) and the Desert Research Institute (DRI) at Reno, the cloud chambers are

cooled by two very different methods. At UMR, thousands of thermoelectric plates are used to try to achieve temperature control and uniformity in the millidegree range. These exquisite requirements are necessitated by an interest in homogeneous-nucleation studies. At DRI, on the other hand, two-phase refrigeration is used, in which coolant in both its liquid and gas phases is pumped through long coils surrounding the chamber. (A single-phase fluid will become considerably warmer as it circulates through the tall chamber, so that uniformity of wall temperature is in doubt, even if unwanted phase change is avoided.) Both of these methods are quite costly and time-consuming to implement. Instead, we adopt the suggestion of W. Finnegan (private communication) to cool the chamber by one-phase refrigeration, as is the procedure implemented for a facility at Colorado State University in Fort Collins. The coolant selected is Lexsol, which itself is not a refrigerant fluid, but (just) a heat-exchange fluid which must be cooled in a heat-exchanger arrangement (shown in Figure 15). The R502 refrigerator system shown in the figure has been operational at TRW for a decade and has capacity of over 3000 kg at 193 K. The design of the heat exchanger, the pumping system, and the manner in which Lexsol circulates through the chamber were tasks of the current project. Major requirements of the experiment are that the chamber walls be reasonably uniform in temperature, and that the gas within the chamber be at about the same temperature as the chamber walls, during the whole cooling process. Implementation of these provisions is intended to preclude any excessive convection in the contents of the cloud chamber during the test interval. Uniformity of temperatures also ensures a uniform distribution of cloud droplets. However, for purposes of inhibiting natural convection, it is desirable to have the top of the chamber wall slightly warmer than the bottom, for example, by 0.5 K over a distance of one meter. A 0.3-K temperature difference between wall and gas seems tolerable (W. Finnegan, private communication). To achieve temperature uniformity in the chamber wall, one requires: (i) large thermal conductivity of the chamber material, and (ii) high flow rate over short path lengths for the coolant. To satisfy (i), aluminum is chosen. To satisfy (ii), the geometry of the coolant flow has to be considered carefully. The traditional geometry for circulation of cooling fluid usually involves a coil helically wrapped around the chamber. The coil, however, entails an exceedingly lengthy

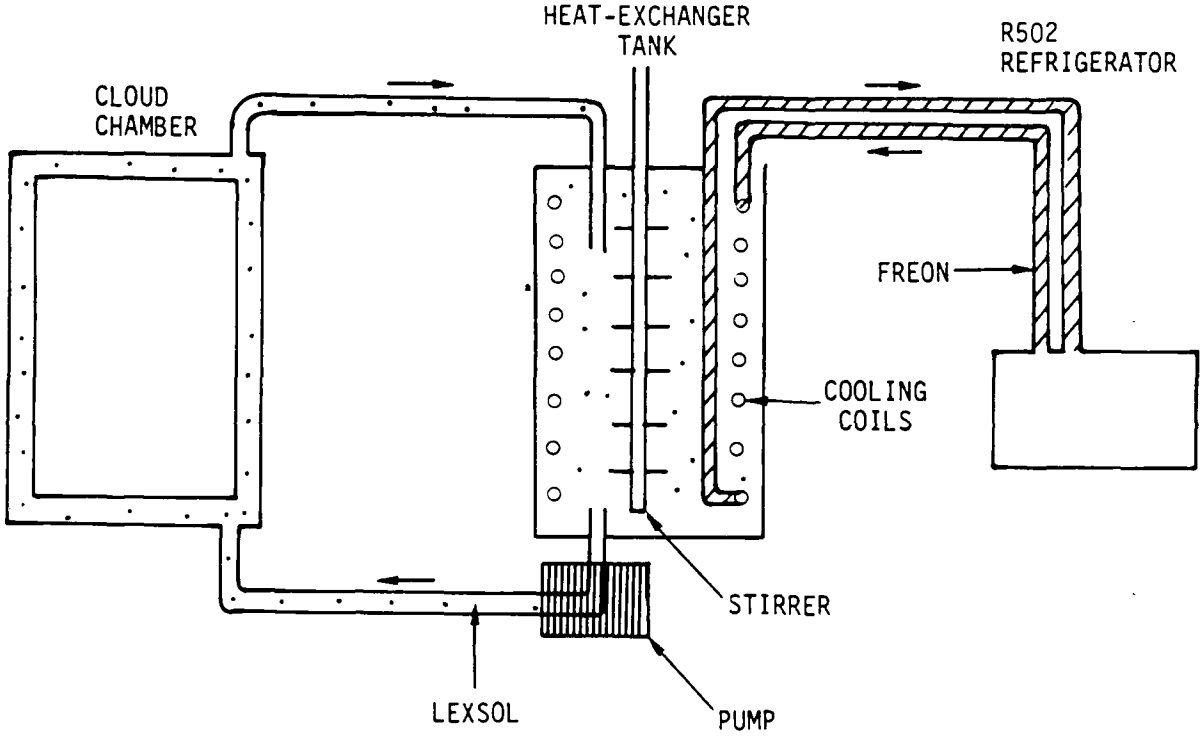

Figure 15. Cooling-system schematic for the cloud chamber.

path, so that the coolant is considerably warmer at the exit than at the entrance. As a result, nonuniform cooling between top and bottom of the chamber would arise. One obvious solution is to use straight tubes instead of coils. Consideration of the straight-tube geometry naturally suggests the double-shelled-cylinder geometry; the coolant passes from the bottom to the top in the annulus between the shells, taken to be thin to reduce thermal inertia (though thick enough structurally to sustain necessary pressure differences across the walls). Calculations show that via a pumping rate of roughly 5×10^{-3} m^3/s, the temperature difference between the top and the bottom of the chamber wall would be about 0.3 K at 253 K.

To achieve uniformity of temperature between the chamber wall and the gas, we let the gas follow the temperature of the wall. The wall has much greater heat capacity than the gas, and the response of the gas temperature to piston expansion (or compression) is almost instantaneous and uniform. The only missing ingredient is a temperature sensor that does not dissipate much heat, but which can sense the (small) temperature difference between the wall and the gas. At UMR, a transistor is used as the temperature sensor in the chamber wall. (Under a constant-collector current, the base-emitter voltage is linearly proportional to the absolute temperature.) The virtue of the transistor, as compared with a thermistor, a thermocouple, or a resistor type of thermometry, is its small heat dissipation, typically 60 μW, equivalent to a 0.03-K rise in temperature in still air. At UMR, a transistor is not used for gas-temperature measurement because of concern that the minute temperature rise may heat the gas. Such heating may be of concern in a homogeneous nucleation study, but should be of no concern for present purposes. Thus, transistor differential thermometry is adopted to monitor the temperature difference between the wall and the gas. The piston is to be moved upward by manual control of a motor drive to minimize the temperature difference between the wall and the gas as the chamber wall is freely cooled by the circulation of Lexsol.

3.2.2 How Is a Cloud to Be Sustained? What Number Density and What Size Should Characterize the Droplets?

In the earliest cloud chambers (Mason 1975), a cloud is formed by rapid expansion, such that the relative humidity momentarily exceeds 100%; at such a relative humidity, cloud droplets start to form around cloud

condensation nuclei (CCN) that are present in the air. If use is made of CCN existing in the air, the range of relative humidity (RH) must be controlled quite accurately between 100% and roughly 101%. If the RH is below 100%, there is no cloud. Above roughly 101%, all the droplets exceed their critical radii and keep growing until they rain (Rogers 1979). If the relative humidity is varied by controlling the temperature, the temperature control has to be highly sensitive and stable. For example, at 273 K, a change in temperature of 0.14 K will cause the RH to change by 1%. Such fine temperature control in a one-phase refrigeration system would be highly difficult, if not impossible. A means of sustaining a stable cloud is to inject an aerosol of NaCl (L. Eaton, private communication). NaCl is hygroscopic and begins to absorb moisture at RH = 78%. Consider the example of a NaCl crystal with a 0.25-μm radius. At RH = 95%, it will have become part of a droplet with a 0.64-μm radius. At RH = 99%, the radius will be 1.2 μm. At 100%, it will be 4.3 μm. Thus, well below 100% RH, droplets of practically interesting size exist and are stable; i.e., their size increases or decreases with RH. This is in contrast to the circumstance with droplets in moist air with RH in excess of 100%. A slight increase of RH in excess of the critical supersaturation will cause the droplets to grow without bound and to rain out. In nature, the forming of droplets on hygroscopic nuclei at a RH below 100% is known as "haze". We observe that haze is stable, and in nature is long-lasting without "fine temperature control".

A cloud in the lower troposphere typically has approximately 1000 droplets/cc, with a mean diameter of droplets of O(10 μm). To simulate the cloud, we would need a similar size and number density for droplets in the cloud chamber. However, 10-μm-sized water droplets have a terminal velocity of about 0.3 cm/s, so that their lifetime in a cloud chamber would be too short for experiments of practically interesting duration. For 2.5-μm droplets, the terminal velocity would be approximately 16 times smaller. In one-half hour, the 2.5-μm droplets would have dropped approximately 40 cm, so that a chamber about 1 m in height would suffice for current purposes. In summary, we decide to form a cloud by injecting a NaCl aerosol with a density of approximately 1000 particles/cc and the particles are to have approximately 0.25-μm-to-0.25-μm radius. Between 95-99% RH, for 99% > RH > 95%, such a NaCl aerosol will form droplets of

approximately 1.25-μm-to-2.5-μm diameter; such droplets should have a sedimentation velocity small enough for a one-half-hour experimentation time. If 10-μm-sized droplets are desired, then the smoke-particle density will have to be increased to compensate for the shorter fallout time of the water droplets, so that sufficient opportunity for collisional interaction is afforded.

3.2.3 How is the Size Distribution of Soot Particles to Be Measured?

There are well-established techniques for particle sizing in aerosol research (Friedlander 1977). They typically involve either the electric-mobility analyzer, the cascade impactor, or the optical particle-size analyzer. The electric-mobility analyzer, while useful for sizes even smaller than 0.1 μm, does not permit fine resolution. Typically there are only four bins/decade. The cascade impactor normally does not perform satisfactorily down to the 0.1-μm-size range. In the last two years, micro-orifice impactors have been developed to be used in that range. However, whether the high velocity of impact (especially in the case of the micro-orifice) will break up the soot chain-aggregates is unknown. Most of the optical particle-size analyzers are predicated upon measuring the total amount of light scattered in the forward direction. They usually are limited to particles larger than 0.3 μm in size.

Independently, in combustion research during the last decade, there has been a development of both ensemble and individual-particle optical-scattering techniques for in-situ measurement in real time of the number density and the mean size of soot particles in a flame or combustion chamber. Most of these techniques entail a combination of two measurements (since there are two outputs, number density and mean size). These techniques are concerned with the multi-angle intensity ratio, the polarization ratio, multiwavelength extinction, and/or the scattering/extinction ratio. An approach based on identification of the scattering/extinction ratio is the one that probably is optimal for particles in the 0.1-μm range. However, all these techniques are beset with two sources of uncertainty: the particles are nonspherical, so that Mie-scattering theory is not strictly applicable; also, the index of refraction is uncertain. The accuracy of any of these techniques probably

is at best to within a factor of two; such accuracy may not be sufficient for our purpose.

Owing to the limitations of all of the above techniques, we chose the most rudimentary of all approaches: particle extraction and then sizing with electron microscopy. The traditional method of extraction usually involves suctioning through an isokinetic probe and then collecting on a membrane filter. However, in membrane filter collection, particle agglomeration may occur around the pores, a phenomenon that we definitely wish to avoid. We thus decided on simply collecting a volume of the sooty gas and letting the soot particles settle gravitationally onto some transmission electron microscopy (TEM) substrates. Particles of 0.1-μm size should settle 2 cm in about 16 hours, so that only an overnight waiting period is required. We have decided on TEM, rather scanning electron microscopy (SEM), because the measurement of 0.1-μm particles would require at least 100,000-x magnification. This resolution is achieved easily by TEM, but is hard (and probably very time consuming) by SEM.

3.2.4 How Is the Optical Extinction by the Smoke to Be Measured?

Optical extinction (Bohren and Huffman 1983) as envisioned in the global-effects context occurs as a result of attenuation over kilometers of optical path length. The same smoke over 1 m of path length in the laboratory effects very little extinction. On the other hand, we ought not increase the smoke density in the laboratory experiment by too much, since coagulation strongly depends on the density of the aerosol constituents. (The collisional frequency between smoke and water droplets is proportional to the product of the number density of the smoke and of the number density of the water droplets.) Thus we have no choice but to devise a method of measuring very small extinction. A quick estimate indicates the level of extinction involved, since (Twomey 1977)

$$I = I_0 \exp(-N\sigma\ell), \tag{8}$$

where I_0 = transmitted light intensity,

I = received light intensity,

N = number density of particles,

σ = extinction cross-section/particle, and

ℓ = path length.

For smoke particles of approximately 0.1-μm size, $\sigma = 0.8\pi r^2$, where r = 0.05 μm. If we adopt $N = 10^5$/cc, ℓ = 1 m, then

$$N\sigma\ell = (10^5)(0.8)\pi(5 \times 10^{-6})^2\ 10^2$$

$$= 6.3 \times 10^{-4}. \qquad (9)$$

Thus intensity would be decreased by less than 0.1%!

One method for measuring small extinction has been applied to identify the visibility range at airports (Knollenberg 1982). It is known as the laser-cavity-extinction photometer, and involves moving one mirror of the laser cavity further from the plasma tube. The space between the plasma tube and the mirror then can be filled with lossy media. If the round-trip gain of the laser through the plasma tube is cancelled by the loss in the (lossy) medium, the laser output decreases from 100% to 0%; i.e., the laser acts as a "loss amplifier". Knollenberg claims that an amplification of 2000 is achievable by use of very clean, highly reflective mirrors. Even if we adopt a loss amplification factor of but 50, the extinction calculated above would become 3.2%, which clearly is measurable. The technique depends on small-loss optics in the optical path. This fact implies that the cloud chamber must have low-loss windows. Fortunately, windows inclined at the so-called Brewster angle are lossless (at least theoretically). Even at 1 degree from the Brewster angle, the loss still is about only 2×10^{-4}. In fact, a Brewster-angle flat slowly rotated through the Brewster angle can be used as a standard by which to calibrate in the extremely low-loss regime. Thus, the arrangement shown in Figure 16 is envisioned for measuring extinction of a 50-mW-HeNe-laser beam by the smoke in the chamber via the following sequence of steps. First, the Brewster-angle flat is placed "in-cavity". It is rotated slowly through the Brewster angle to establish laser-output power as a function of in-cavity loss. Then the Brewster-angle flat is removed and an evacuated cloud chamber is moved into place. Extinction is measured. The chamber is filled with air and smoke. Extinction again is measured. At the end of

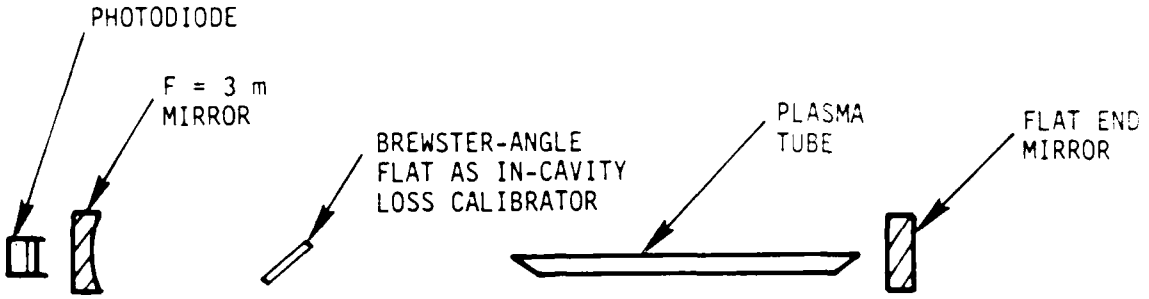

(a)

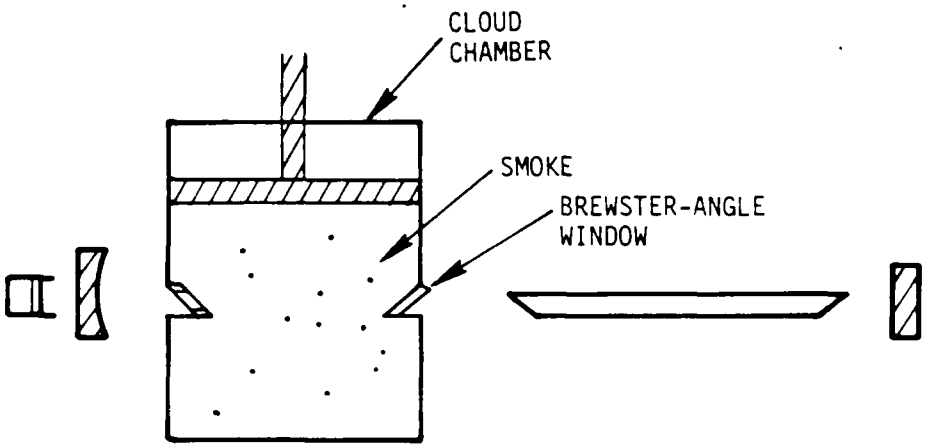

(b)

Figure 16. Extinction-of-light-by-smoke measurement using the laser-cavity-extinction-photometer method: (a) laser output versus in-cavity-loss calibration by a Brewster-angle flat; (b) cloud chamber in place for an actual extinction measurement.

the experiment [i.e., after smoke has been confined with the cloud for (say) one-half hour and the cloud is evaporated by compression], the above steps are executed in reverse order. Measuring low-level extinction admittedly is a most difficult task, and probably will be the most difficult part of the experiment.

3.3 HARDWARE DESCRIPTION.

3.3.1 Refrigeration.

TRW presently owns a two-stage R502 refrigeration system with capacity of 3000 kg at 193 K (as previously noted) and of 1300 kg at room temperature.

The heat-exchange system designed for the cloud-chamber experiment is a secondary-brine-refrigeration system, with Lexsol as the secondary brine. Temperature is controlled through the use of a fast-pulsed solenoid to regulate the R502 bypass, which operates down to a preselected temperature and then switches to straight refrigeration. This arrangement permits sufficient control from room temperature down to 208 K. A 0.57-m^3 tank is used for the Lexsol. It is pumped by canned rotor pumps (without seals and magnetically coupled) at 5×10^{-3} m^3/s for the annulus of the cloud chamber, and at 6.3×10^{-4} m^3/s for the piston and bottom plate of the cloud chamber. The whole system is regulated by a microprocessor-based temperature control that effects a predetermined program of up to eight steps of any temperature ramp or soak (within the system capacity). For example, if the start, stop temperatures and the temperature ramp time are preset, the control proceeds without the need for intervention. To ensure a minimum temperature gradient within the Lexsol tank, a high-velocity-stirring device is installed. Bypass valves also are installed on the pumps to facilitate flow control.

3.3.2 Cloud Chamber.

The cloud chamber is a double-shelled cylinder of 6061T6 aluminum (Figure 17). Its inner dimensions are 61 cm in diameter and 122 cm in length. The two shells each are 1.27 cm in thickness, with 1.27-cm (annular) spacing between. The cylinders were made by rolling a 1.27-cm sheet of aluminum to form a cylinder, then butt-welded and heat treated to release the stress. The inner cylinder then was bored. There is a total

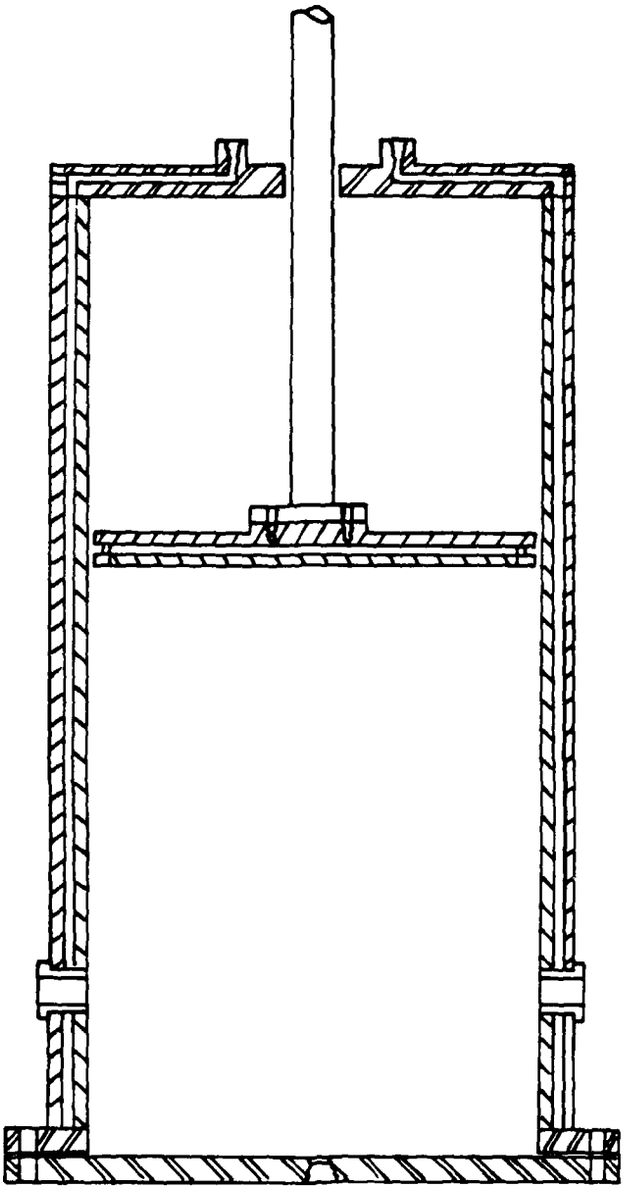

Figure 17. Cross-sectional view of the cloud chamber. The interior dimensions are diameter of 61 cm and length of 122 cm.

of seven ports around the chamber (near the base, where the cloud is likely to be sustained the longest). One pair is for cloud-droplet-size measurement. One pair is for extinction measurement. The alignment of this pair is quite critical because of the Brewster-angle-window requirement. One port is for the smoke-sampling probe. The remaining pair is for either scattering measurement or observation. There also are six holes close to the bottom of the chamber for pumping the Lexsol coolant into the chamber annulus, from which the coolant is pumped out through the top. Remaining holes in the chamber are for installation of transistor thermometers and absolute thermometers.

The piston is a hollow plate of aluminum. It has a stroke of roughly 77 cm, from roughly 30 cm from the bottom of the chamber to 107 cm above the bottom. Its exact location is monitored by a linear position indicator. The piston is driven by a lead screw, powered by a 560-W variable-speed motor reduced by a gear ratio of 160 to 1. The piston can move as slowly 0.056 mm/s or as fast as 0.51 mm/s. The piston seal is a polypak seal made by Parker. The seal has two lips with a nitrile O-ring as its "spring". It can operate at temperatures as low as 218 K and is designed to serve better than O-rings in low-speed, long-stroke operations. The piston is cooled actively by pumping Lexsol through radially drilled holes.

The bottom plate of the chamber also is cooled actively by pumping Lexsol through radially drilled holes.

Pressure in the chamber below the piston is monitored by a Heise absolute-pressure gauge. The differential pressure between the chamber above the piston and the chamber below the piston is monitored by a Magnehelic gauge with ±38-cm-of-water range. For equilization of the pressure between the two sides when the piston is being raised for expansion, the evacuation and pumping circuit presented in Figure 18 has been installed.

The whole chamber is enwrapped by a 5-cm thickness of Armaflex for thermal insulation. A frame has been constructed with rails on top. The chamber is suspended from two plates which move on the rails. This provision enables the chamber to be moved in and out of the optical-table area, in which the extinction measurements are to be made. A photograph of the chamber suspended in the frame is provided as Figure 19.

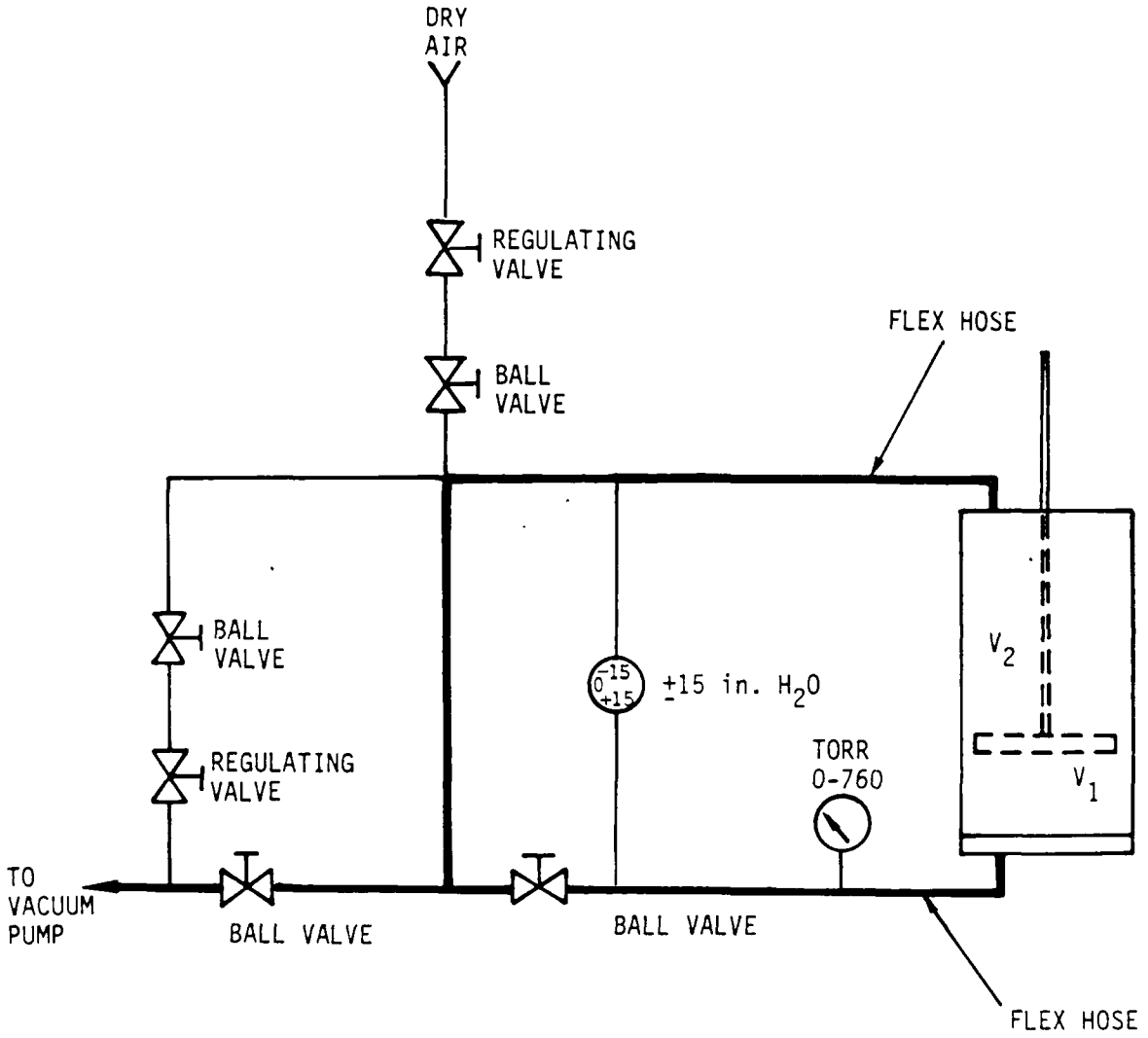

Figure 18. Pumping and filling circuit for the cloud chamber. (15 in. $H_2O \equiv 3.75$ kPa; 760 torr $\equiv 10^2$ kPa.)

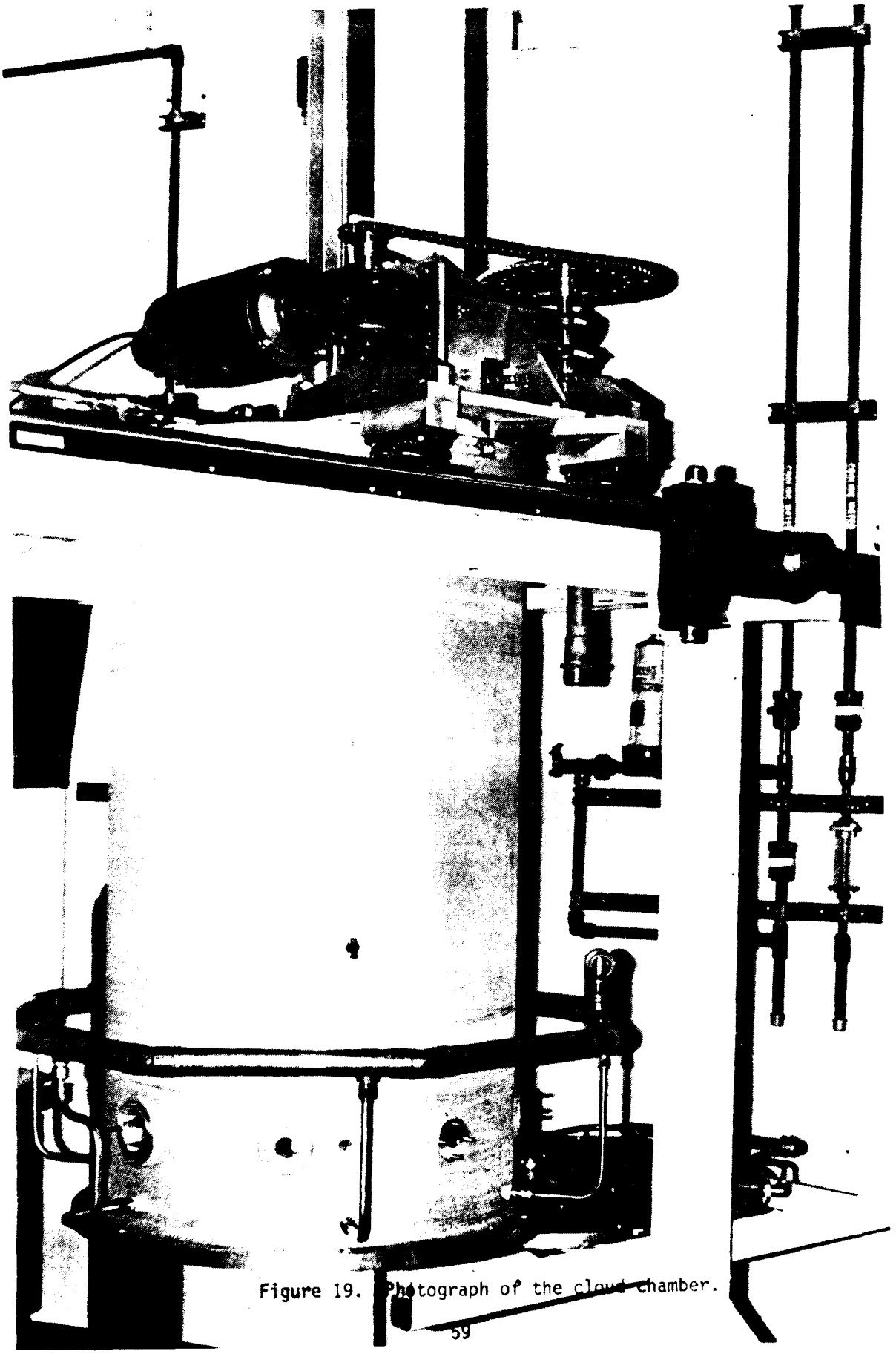

Figure 19. Photograph of the cloud chamber.

3.3.3 Air, Humidity, Aerosol, and Smoke Introduction.

In most cloud-chamber and aerosol-research facilities, the introduction of air, humidity and aerosol into the test chamber involves considerable plumbing and circuitry. Such extensive conduits are required to furnish a continuous flow for filtering and drying air, and then for humidifying the air to the desired RH, and for aerosol generation and dilution to the desired concentration. The present experiment processes "working fluid" in a "batch" mode, rather than in a "continuous" mode. Consequently, the approach is to meter precisely the proper amount of dry air, humidity, salt aerosol, and smoke before they are introduced into the cloud chamber.

For dry filtered air, we use bottled dry air, the dew point of which is 223 K. This air then is passed through a high-efficiency cartridge air filter before introduction into the chamber.

For water-vapor input, conventionally, dry air is passed over a container with liquid water at an elevated temperature. The exiting air is saturated at that temperature. It then is diluted to the desired RH. This procedure is too cumbersome for our purpose. We simply inject the desired amount of filtered liquid water into the chamber before the start of the experiment. For example, if the final temperature desired in the experiment is 278 K and the final height of the piston above the bottom is 61 cm, the amount of water needed to reach 100% humidity at 278 K is 1.21 g. Water is injected via syringe through a filter, by the arrangement shown in Figure 20.

The procedure for aerosol generation and introduction is sketched in Figure 21. Salt solution is atomized in a Collision atomizer to form solution droplets of about 2.0-μm diameter. This preparation then is passed through a TSI diffusion dryer to remove the water, so that a salt aerosol with particles of about 0.2-μm-to-0.3-μm diameter remains. These particles then are passed through a neutralizer (to neutralize the electrical charges that usually result from the atomization process). The neutralized aerosol is transported to a metering cylinder. After the flow has steadied, the metering cylinder is sealed to enclose the proper volume of aerosol, which then is pumped into the chamber.

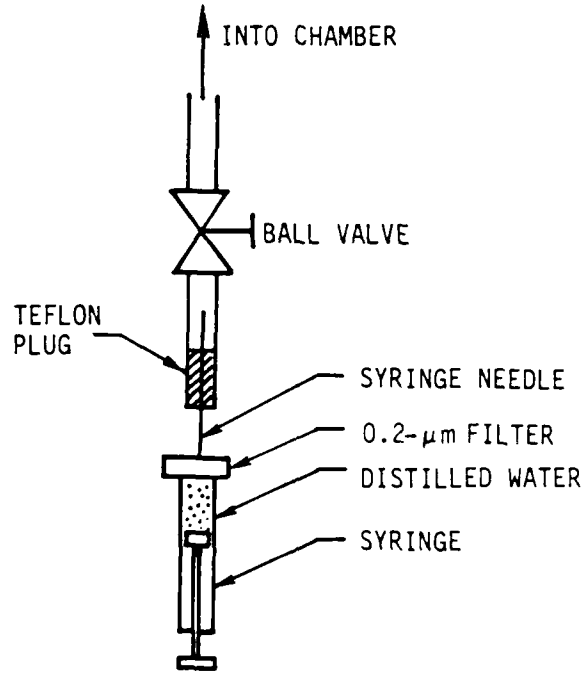

Figure 20. Method of water injection into the cloud chamber.

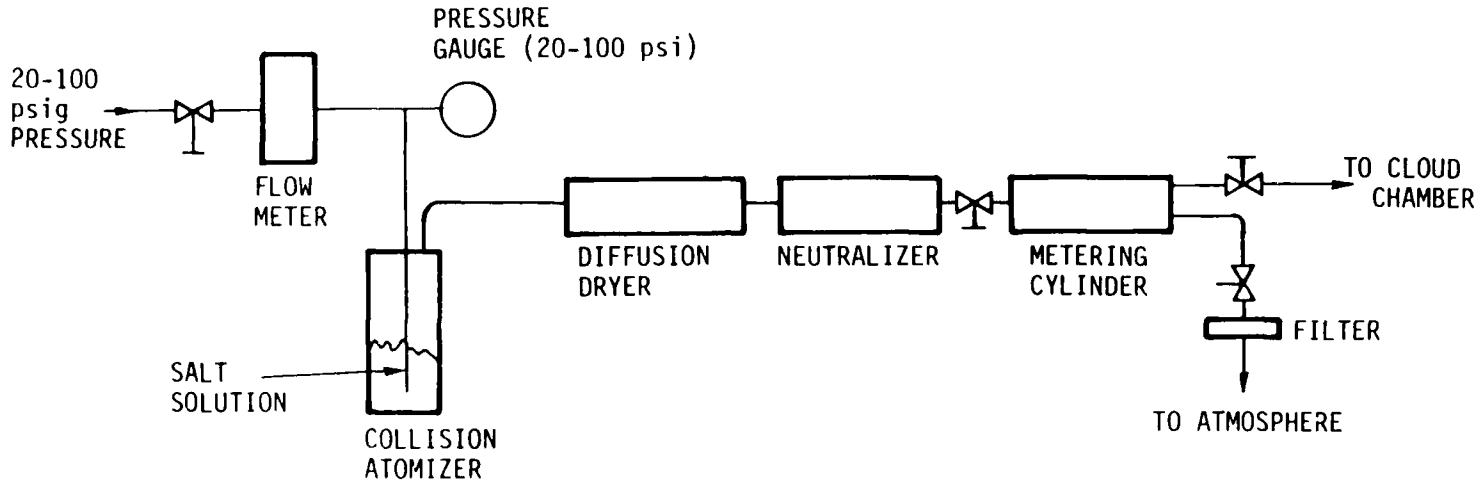

Figure 21. Salt-aerosol generation and injection system. (1 psi ≡ 6.89 x 10^3 Pa.)

The procedure for smoke generation and introduction is sketched in Figure 22. For the initial trials, acetylene is to serve as the fuel (though mainly polymeric fuels are to be burned to furnish smoke for the data of interest). The acetylene is to be combusted in a Bunsen burner, the smoke being captured by a funnel located 15 cm above the flame and then being passed through a coil to remove some of the moisture. The smoke is conveyed into a "metering" cylinder with two windows, to that a 2-mW HeNe laser beam can be passed through the contents to assess (via extinction) that the proper density of smoke has been captured. The smoke then is pumped into the chamber.

3.4 INSTRUMENTATION DESCRIPTION.

3.4.1 Temperature Measurement.

There are two absolute thermometers and five pairs of differential thermometers in the chamber. The two absolute thermometers are IC devices in TO-5 cans, made by Analog Devices as item AD930. The operation of the absolute thermometers is predicated on the principle that, when a transistor is operated at constant collector current, the base-emitter voltage is linearly proportional to the absolute temperature. The device acts as a two-terminal current source with a sensitivity of 1 mV/K. With two-point trimming, it can have an accuracy of 0.05 K from 298 K to 218 K.

The absolute-thermometer type AD930 is easy to use. However, because it incorporates both the sensing transistors and the rest of the circuitry together in the same chip, it dissipates more heat (about 3 mW) than is desirable. Hence it can be used to monitor wall temperature only, not gas temperature.

The differential-thermometry pairs basically are predicated on the same principle as the AD930. However, only the sensing transistor is placed at the site of measurements, while the rest of the circuitry is placed outside the chamber. As a result, less heat (approximately 60 μW per transistor) is generated. The circuitry for the differential thermometry is presented in Figure 23. The sensitivity is about 120 mV/K.

3.4.2 Cloud-Droplet-Size Measurements.

The cloud-droplet-size measurement is depicted in Figure 24. It involves a 2-mW HeNe laser as a light source. The receiving optics

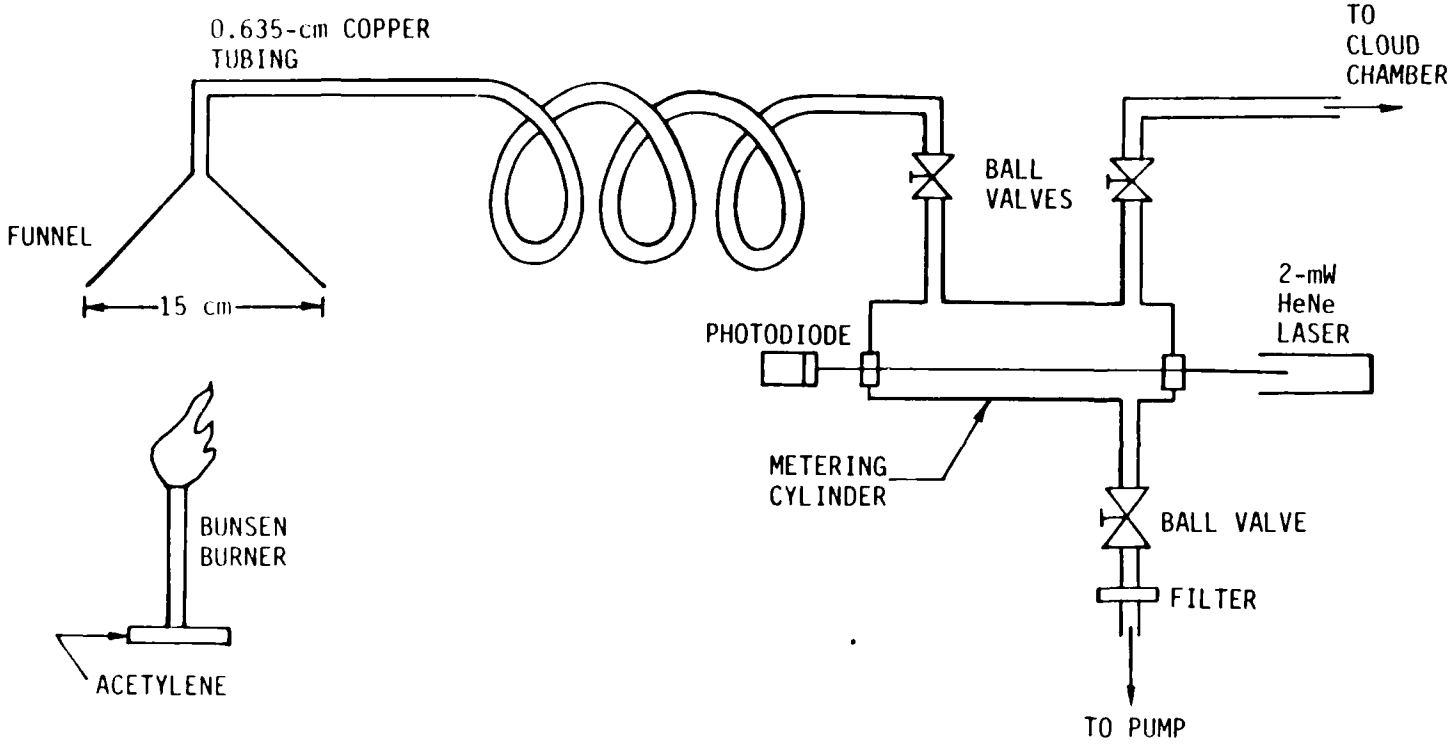

Figure 22. Smoke collection and injection system.

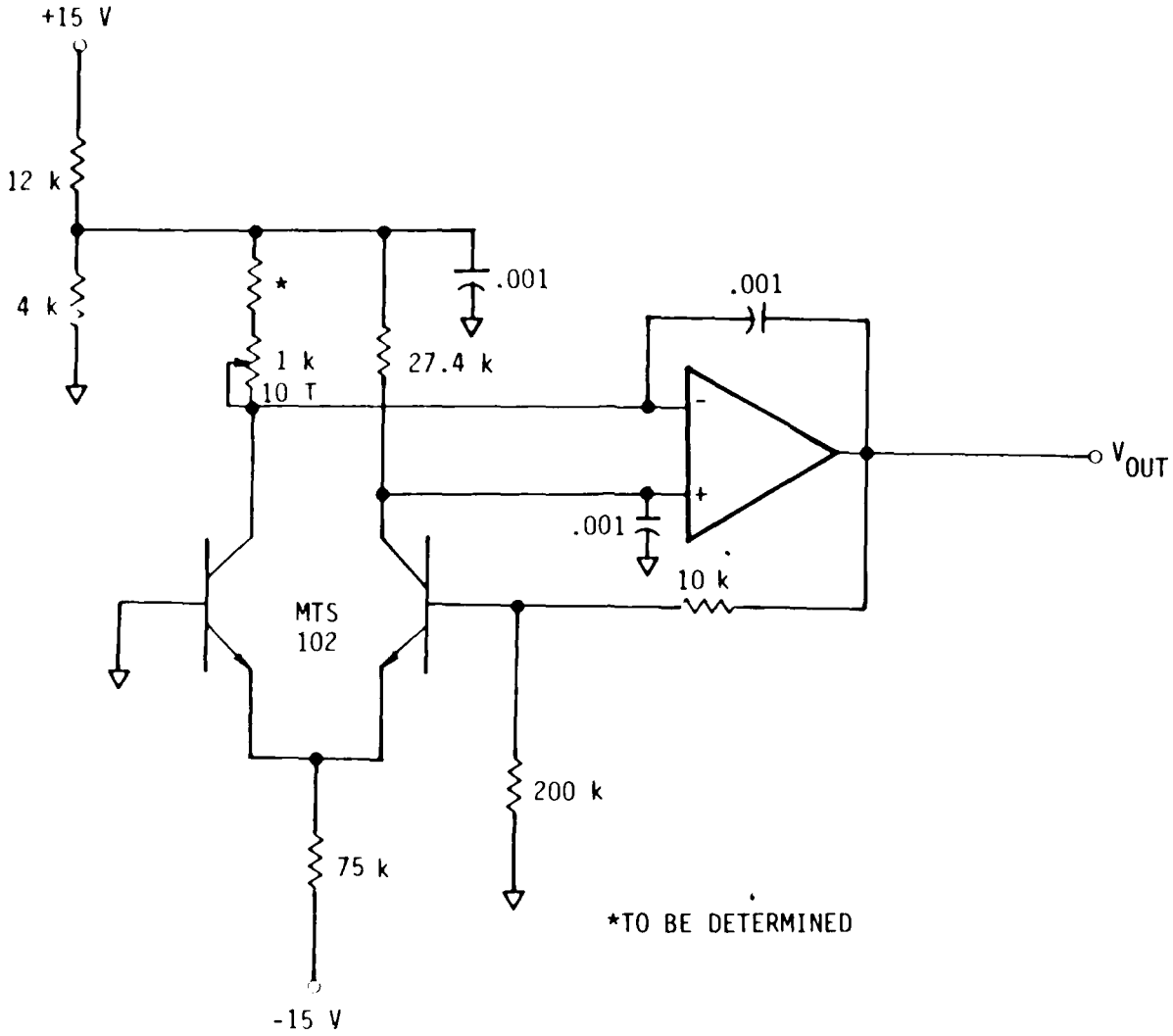

Figure 23. Schematic for transistor differential thermometry. (The notation k for resistors implies kΩ; the notation T for potentiometer implies turns; absence of notation near capacitors implies μf; and MTS 102 denotes a particular Motorola transistor to be used for this purpose.)

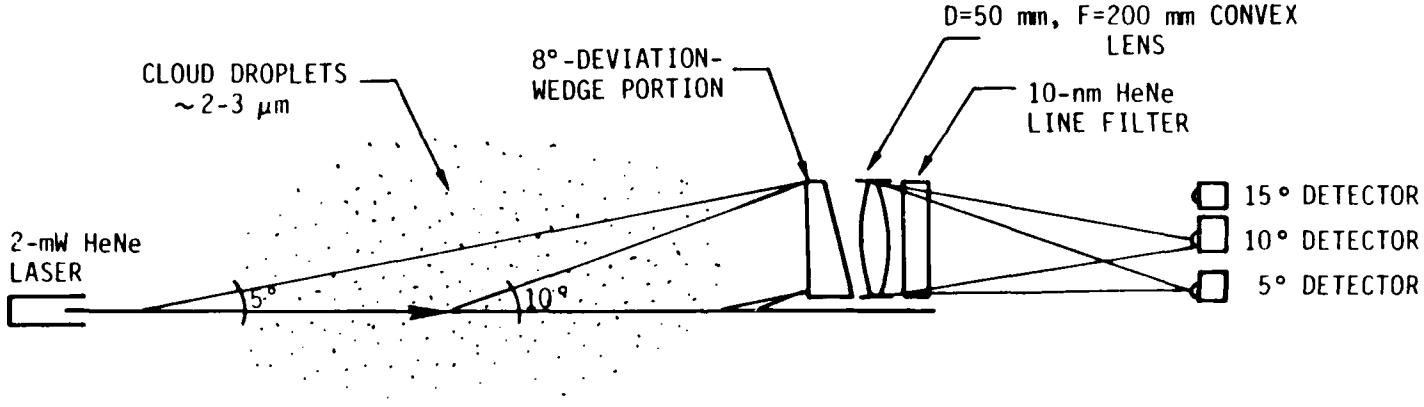

Figure 24. Cloud-droplet-size-measurement system, using 5°, 10°, 15° Fraunhoffer diffraction in the forward direction.

consists of an 8-degree deviation wedge; a plano-convex lens with aperture D = 50 mm and focal length F = 200 mm; a 10-nm HeNe line filter; and three ultralow-noise-photodiode preamplifiers from EG&G. That light (from the laser) which is scattered at 5 degrees, 10 degrees, and 15 degrees near the forward direction is focused by the lens onto the respective photodiode preamplifiers. In the forward direction, the index of refraction is not a significant factor, and Fraunhoffer diffraction approximates Mie scattering. The ratio of the scattering intensities for any pair of angles permits the determination of the mean size of the droplets.

3.4.3 Soot Sampling.

The soot-sampling probe is depicted in Figure 25. Basically it is a little piston-and-cylinder arrangement connected to the chamber with a long-nose probe. As noted earlier, ideally sampling is executed "isokinetically". In still air that implies intruding into the chamber with a "grabber" and capturing a sample. Fortunately, soot particles are so small that they follow the flow without slip at low velocity, even if sampling is not isokinetic. The adopted method of suctioning through a long-nose probe is easy to fabricate. The long-nose probe is situated outside the chamber until the time of sampling, at which point the probe is pushed in towards the center of the chamber.

After sampling, the cylinder containing the extracted sample can be detached from the valve. An identical cylinder then can be attached to the valve to perform another, subsequent sampling. The piston draws only 2 cm. The 0.1-μm soot particles in the extracted volume should settle in less than 16 hours. Three 3-mm-diameter TEM 200-mesh copper grids with Collodian-film substrates are placed in the center of the piston to receive the soot particles.

3.4.4 Soot Extinction Measurement.

The general extinction-measurement concept has been discussed earlier. In more detail, the laser is a Spectra Physics 125 HeNe laser rated at 50 mW. This laser has a removable mirror mount for in-cavity-experimentation purposes. We have performed bench tests of the concept (Knollenberg 1982) with different outcoupling mirrors and have found satisfactory results. We adopted the confocal geometry, which is the most stable against mirror

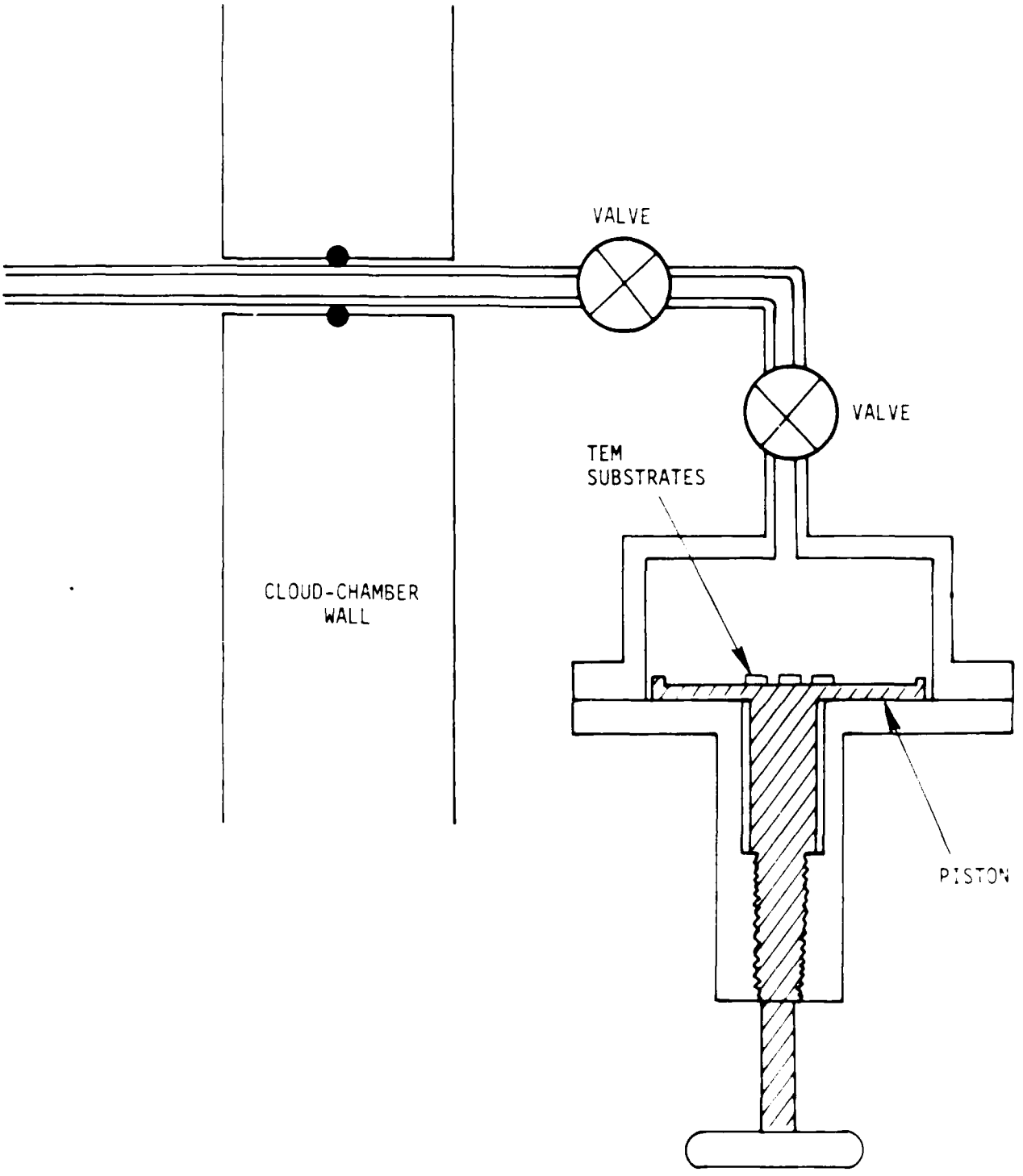

Figure 25. Schematic drawing of the smoke-sampling probe (in the fully retracted position).

misalignment, a most important consideration when mirrors are moved apart (Ralph Wuerker, private communication). Mirror-thermal-motion drift is the most significant source of laser-output-power fluctuation. With the Spectra Physics mirror mount, we found that after warming, fluctuation in output is about 0.3% to 0.5% over 10 minutes. Obviously, the signal has to exceed this fluctuation to be detectable. Two separate outcoupling mirrors have been tried, one being a 3-m-f.l., 2.6% outcoupling, and the other being a 3-m-f.l., 0.9% outcoupling. The result for the latter is shown in Figure 26. Here the output power is plotted against in-cavity loss, in this case established by a rotating Brewster-angle flat. It can be seen that a "loss-enhancement" factor of about 70 can be achieved without meticulous cleaning of the mirrors. Together with the 0.3% output-fluctuation noise, the result implies that the noise-equivalent absorption for the system is approximately 0.3%/70 = 0.004%, which already quite suffices for our objectives.

3.4.5 Preliminary Checkouts.

The following preliminary checkouts were performed.

- With respect to cloud formation at room temperature via use of pre-existing CCN, liquid water was injected into the chamber. After a half hour, the meter for relative humidity indicated that the chamber was close to 100% RH. A 2-mW HeNe laser beam was directed through the chamber for purposes of cloud visualization. The beam was not observable at 45 degrees and 135 degrees. When the piston was moved upward by the motor, the beam immediately became visible. After about one minute, the beam slowly disappeared again, an indication of the difficulty of maintaining a long-lasting cloud via pre-existing CCN.
- With respect to cloud formation at room temperature via use of NaCl aerosol, a 0.25-μm-radius NaCl aerosol was injected into the chamber. The laser beam again became visible and stabilized after a few minutes. After 20 minutes, the beam still was quite bright, an indication that NaCl injection is indeed a means by which to generate a long-lasting cloud.

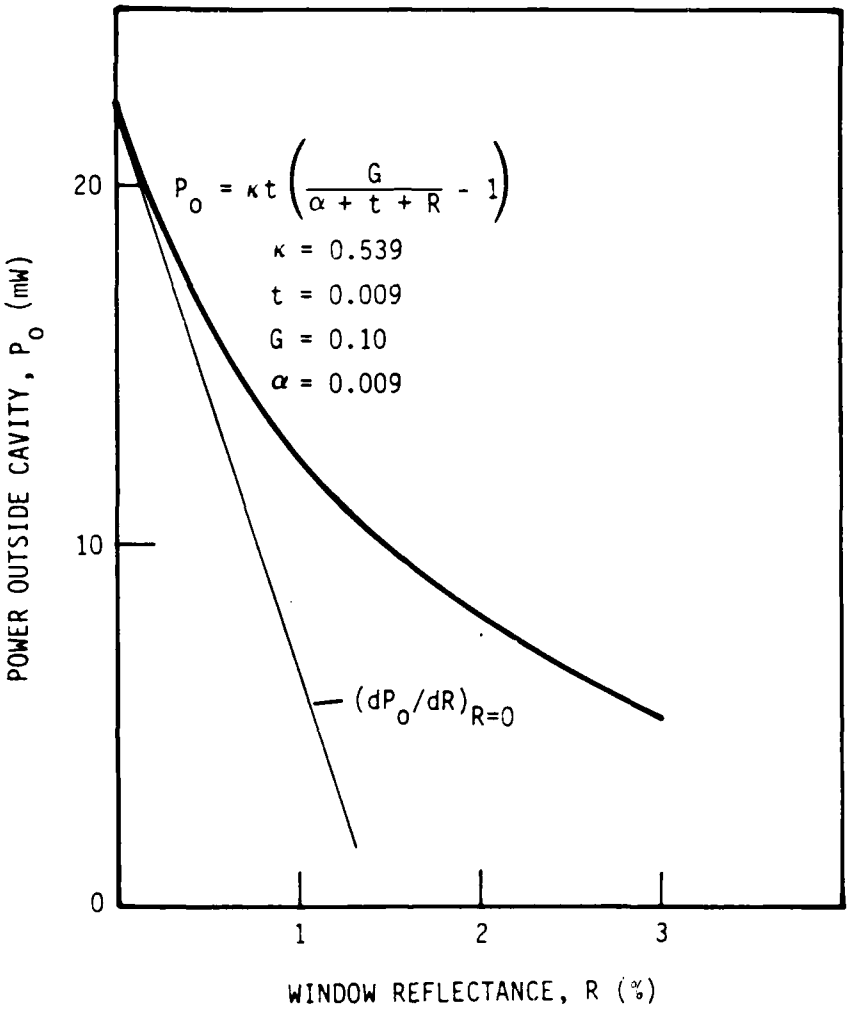

Figure 26. Laser-output power versus in-cavity loss owing to reflectance of the Brewster-angle flat of 2-mm-thick fused silica (as it deviates from the Brewster angle). The end mirror of the laser has radius 3 m and 0.9% transmittance. The empirical formula for the laser-output power versus loss is manufacturer-supplied and has been confirmed by trial. The slope of the curve as the in-cavity loss $R \to 0$ yields the asymptotic loss-amplifying factor (or "efficiency") of the design as almost 70.

- o The heat-exchanging tank was filled with Lexsol and cooled to 233 K by use of the microprocessor-based control system. It then was maintained at 233 K for more than one hour before refrigeration was terminated. After 24 hours, the heat exchanging tank still was at 260 K, an indication of very little heat leakage into the system.
- o Lexsol was introduced from the heat-exchanging tank into the cloud chamber. The temperature-control system was programmed to cool the whole system from room temperature to 287 K, to "soak" at 287 K for 20 minutes, then to cool the system to 277 K in 10 minutes, and to "soak" for another 15 minutes. The system performed as expected with no leaks. The temperature variation during the "soaking" periods was less then 1 K (the resolution of the panel meter).

3.5 EXPERIMENTAL TESTS AND RECOMMENDATIONS.

It is recommended that a systematic parametric investigation of wet coagulation and wet precipitation as simulated in the above-described cloud chamber be carried out, once three tests to demonstrate the capabilities of the apparatus are executed successfully.

The first test is to demonstrate that a haze at relative humidity of nearly 100% can be stabilized for at least one-half hour at (say) 278 K. In fact, already such a test has been performed by introduction into clean air at room temperature of less than a saturation amount of water and of about 10^3 salt particles per cubic centimeter of size 0.2 μm to 0.3 μm. Circulation of coolant in the chamber walls then lowered the temperature of the chamber contents to 278 K, such that the relative humidity was 95%-100%, and a laser beam indicated first the onset of condensation at above 280 K and then the persistence of droplets for over a half hour at 278 K. The second test is to repeat the first test, but with over 10^4 smoke particles per cubic centimeter introduced prior to the salt particles and water, so that a before-cloud/after-cloud comparison of the smoke-particle-size distribution can be made (say) via sampling and transmission electron microscopy. The third test is a slightly different test of wet coagulation from test two. Entirely at room temperature, after the smoke is introduced, enough water is added to saturate the air at ambient temperature, so that a small pool of liquid water exists. Again,

the effect on smoke-particle-size distribution of the coexistence of the smoke and the water-droplet aerosols for (say) a half hour is to be measured. This test conceptually could be executed at any temperature down to 273 K by the introduction of the water after cooling; below 273 K the use of a brine solution to preclude freezing of the condensed water phase should be considered. Tests two and three remain to be attempted, but expectation is for success. Aside from the possible desirability of slightly better coolant circulation through the cylinder base, the chamber indeed seems to have been well designed and constructed to serve wet-coagulation-of-smoke simulations.

SECTION 4

LIST OF REFERENCES

Anderson, H. E., and Rothermel, R. C. 1965 Influence of moisture and wind upon the characteristics of free-burning fires. Tenth Symposium (International) on Combustion, 1009-1019. Pittsburgh, PA: Combustion Institute.

Bohren, C. F., and Brown, G. M. 1981 Once in a blue moon. Weatherwise 34, 129-130.

Bohren, C. F., and Huffman, D. R. 1983 Absorption and Scattering of Light by Small Particles. New York, NY: John Wiley.

Brown, J. K. 1972 Field test of a rate-of-fire-spread model in slash fuels. Intermountain Forest and Range Experiment Station Research Paper INT-116. Ogden, UT: Forest Service, U.S. Dept. of Agriculture.

Byram, G. M., Clements, H. B., Bishop, M. E., and Nelson, Jr., R. M. 1966 An experimental study of model fires. Macon, Georgia: Southern Forest Fire Laboratory, Forest Service.

Cheney, N. P. 1981 Fire behavior. Fire in the Australian Biota, 151-175. Canberra, Australia: Australian Academy of Science.

Committe on the Atmospheric Effects of Nuclear Explosions 1985 The Effects on the Atmosphere of a Major Nuclear Exchange. Washington, DC: National Academy Press.

Emmons, H. W. 1965 Fundamental problems of the free burning fire. Tenth Symposium (International) on Combustion, 951-964. Pittsburgh, PA: Combustion Institute.

Emmons, H. W., and Shen, T. 1971 Fire spread in paper arrays. Thirteenth Symposium (International) on Combustion, 917-926. Pittsburgh, PA: Combustion Institute.

Fang, J. B. 1969 An investigation of the effect of controlled wind on the rate of fire spread. Ph.D. thesis, Dept. of Chemical Engineering. Fredericton, Canada: U. of New Brunswick.

Fang, J. B., and Steward, F. R. 1969 Flame spread through randomly packed fuel particles. Combust. Flame 13, 392-398.

Fons, W. L. 1946 Analysis of fire spread in light forest fuels. J. Agricultural Res. 72, 93-121.

Fons, W. L., Clements, H. B., and George, P. M. 1963 Scale effects on propagation rate of laboratory crib fires. Ninth Symposium (International) on Combustion, 860-866. New York, NY: Academic.

Fleeter, R., Fendell, F., Cohen, L. M., Gat, N., and Witte, A. B. 1984 Laboratory facility for wind-aided firespread along a fuel matrix. Combust. Flame 57, 289-311.

Friedlander, S. K. 1977 Smoke, Dust and Haze--Fundamentals of Aerosol Behavior. New York, NY: John Wiley.

Glasstone, S., and Dolan, P. J. 1977 The Effects of Nuclear Weapons, 3rd ed. Washington, DC: U.S. Department of Defense & U.S. Department of Energy.

Goldberg, E. D. 1985 Black Carbon in the Environment--Properties and Distribution. New York, NY: John Wiley.

Gostintsev, Y. A., and Sukhanov, L. A. 1978a Convective column above a linear fire in a homogeneous isothermal atmosphere. Combust., Explosions, & Shock Waves 13, 570-578.

Gostintsev, Y. A., and Sukhanov, L. A. 1978b Interaction of convective columns above linear sources of heat. Combust., Explosions, & Shock Waves 14, 60-64.

Gostintsev, Y. A.. and Sukhanov, L. A. 1979 Interaction between a convective column and the wind above a linear fire in a polytropic atmosphere. Combust., Explosions, & Shock Waves 14, 452-455.

Grishin, A. M., Gruzin, A. D., and Gruzina, E. E. 1985 Aerodynamics and heat exchange between the front of a forest fire and surface layer of the atmosphere. J. Appl. Mech. Tech. Phys. 6, 91-96.

Hottel, H. C., Williams, G. C., and Steward, F. R. 1965 The modeling of firespread through a fuel bed. Tenth Symposium (International) on Combustion, 997-1007. Pittsburgh, PA: Combustion Institute.

Hwang, C. C., and Xie, Y. 1984 Flame propagation along matchstick arrays on inclined base boards. Combust. Sci. Tech. 42, 1-12.

Knollenberg, R. G. 1982 A laser cavity extinction photometer for measurements of extinction coefficient and visual range. Light Absorption by Aerosol Particles, 65-69. Hampton, VA: Spectrum.

Luke, R. H., and McArthur, A. G. 1977 Bushfires in Australia. Canberra, Australia: Australian Govt. Printing Service.

Luti, F. M. 1980 Transient flow development due to a strong heat source in the atmosphere. Part 1: uniform temperature source. Combust. Sci. Tech., 23, 163-175.

Luti, F. M. 1981 Some characteristics of a two-dimensional starting mass fire with cross flow. Combust. Sci. Tech. 26, 25-33.

Mason, B. J. 1957 The Physics of Clouds. Oxford, England: Clarendon.

Mason, B. J. 1975 Clouds, Rain and Rainmaking, 2nd ed. Cambridge, England: Cambridge University.

Nelson, R. M., Jr., and Adkins, C. W. 1986 Flame characteristics of wind-driven fires in surface fuels. Can. J. For. Res., to appear.

Miller, R. A. 1970 Flame propagation in two-dimensional matchstick arrays. Report, Dept. of Aerospace & Mechanical Sciences. Princeton, NJ: Princeton U.

Prahl, J. M., and T'ien, J. S. 1973 Preliminary investigation of forced convection on flame propagation along paper and matchstick arrays. Combust. Sci. Tech. 7, 271-282.

Putnam, A. A. 1965 A model study of wind-blown free-burning fires. Tenth Symposium (International) on Combustion, 1039-1046. Pittsburgh, PA: Combustion Institute.

Roessler, D. M., and Faxvog, F. R. 1979 Optoacoustic measurement of optical absorption in acetylene smoke. J. Opt. Soc. Amer. 69, 1699-1704.

Rogers, R. R. 1979 A Short Course in Cloud Physics, 2nd ed. New York, NY: Pergamon.

Rothermel, R. C., and Anderson, H. E. 1966 Fire spread characteristics determined in the laboratory. Research Paper INT-30. Ogden, UT: Intermountain Forest & Range Experiment Station, Forest Service.

Slinn, W. G. N. 1984 Precipitation scavenging. Atmospheric Science and Power Production, 466-532. Springfield, VA: Technical Information Center, U.S. Department of Energy.

Steward, F. R. 1974 Fire spread through a fuel bed. Heat Transfer in Fires: Thermophysics, Social Aspects, Economic Impact, 315-378. Washington, DC: Scripta.

Steward, F. R., and Tennankore, K. N. 1981 The measurement of the burning rate of an individual dowel in a uniform fuel matrix. Eighteenth Symposium (International) on Combustion, 641-646. Pittsburgh, PA: Combustion Institute.

Steward, F. R., and Waibel, R. T. 1973 Flame spread through uniform fuel matrices. Report, Fire Science Center. Fredericton, Canada: U. of New Brunswick.

Steward, F. R., Wuest, L. J., and Waibel, R. T. 1977 Some characteristics of fires within uniform fuel matrices. Heat Transfer Div. Paper 77-HT-71. New York, NY: American Society of Mechanical Engineers.

Thomas, P. H. 1963 The size of flames from natural fires. Ninth Symposium (International) on Combustion, 844-858. New York, NY: Academic.

Thomas, P. H. 1971 Rates of spread of some wind-driven fires. Forestry 44, 155-175.

Twomey, S. 1977 Atmospheric Aerosols. New York, NY: Elsevier.

Van Wagner, C. E. 1968 Fire behaviour mechanisms in a red pine plantation: field and laboratory evidence. Publication 1229. Chalk River, Ontario, Canada: Petawawa Forest Experiment Station, Dept. of Forestry and Rural Development.

Vogel, M., and Williams, F. A. 1970 Flame propagation along matchstick arrays. Combust. Sci. Tech. 1, 429-43.

DISTRIBUTION LIST

DEPARTMENT OF DEFENSE

DEFENSE INTELLIGENCE AGENCY
ATTN: DB-6E1 J REMPLE
ATTN: DB-6E2 C WIEHLE
ATTN: RTS-2B
ATTN: WDB-4CR

DEFENSE NUCLEAR AGENCY
ATTN: OPNS
ATTN: RAAE
2 CYS ATTN: TDTR
4 CYS ATTN: TITL

DEFENSE TECHNICAL INFORMATION CENTER
12 CYS ATTN: DD

FIELD COMMAND DEFENSE NUCLEAR AGENCY
ATTN: FCTXE
ATTN: FTTD W SUMMA

JOINT STRAT TGT PLANNING STAFF
ATTN: JKCS

DEPARTMENT OF ENERGY

LAWRENCE LIVERMORE NATIONAL LAB
ATTN: L-442, J BACKOVSKY
ATTN: N ALVAREZ
ATTN: R PERRETT

LOS ALAMOS NATIONAL LABORATORY
ATTN: DR. D CAGLIOSTRO

OTHER GOVERNMENT

DEPARTMENT OF COMMERCE
ATTN: H BAUM
ATTN: R LEVINE

DIRECTOR, FFASR
ATTN: C CHANDLER

FEDERAL EMERGENCY MANAGEMENT AGENCY
ATTN: H TOVEY
ATTN: OFC OF RSCH/NP H TOVEY

DEPARTMENT OF DEFENSE CONTRACTORS

CALIFORNIA RESEARCH & TECHNOLOGY, INC
ATTN: M ROSENBLATT

CARPENTER RESEARCH CORP
ATTN: H J CARPENTER

CHARLES SCAWTHORN
ATTN: C SCAWTHORN

FACTORY MUTUAL RESEARCH CORP
ATTN: R FRIEDMAN

IIT RESEARCH INSTITUTE
ATTN: H NAPADENSKY

INSTITUTE FOR DEFENSE ANALYSES
ATTN: L SCHMIDT

KAMAN SCIENCES CORP
ATTN: E CONRAD

KAMAN TEMPO
ATTN: DASIAC

KAMAN TEMPO
ATTN: DASIAC

MISSION RESEARCH CORP
ATTN: J BALL

MODELING SYSTEM, INC
ATTN: G BERLIN

NOTRE DAME DU LAC, UNIV OF
ATTN: T J MASON

PACIFIC-SIERRA RESEARCH CORP
ATTN: H BRODE, CHAIRMAN SAGE
ATTN: R SMALL

R & D ASSOCIATES
ATTN: D HOLLIDAY
ATTN: F GILMORE
ATTN: R TURCO

RAND CORP
ATTN: P DAVIS

RAND CORP
ATTN: B BENNETT

SCIENCE APPLICATIONS INTL CORP
ATTN: M DRAKE
ATTN: M MCKAY

SCIENCE APPLICATIONS INTL CORP
ATTN: J COCKAYNE

SCIENTIFIC SERVICES, INC
ATTN: C WILTON

SRI INTERNATIONAL
ATTN: G ABRAHAMSON

STAN MARTIN ASSOCIATES
ATTN: S MARTIN

SWETL, INC
ATTN: T PALMER

TRW SPACE & DEFENSE
2 CYS ATTN: D S W KWOH
2 CYS ATTN: B M LAKE
2 CYS ATTN: C T HSU
2 CYS ATTN: F FENDELL
2 CYS ATTN: G F CARRIER
2 CYS ATTN: K L BEACH
2 CYS ATTN: M F WOLFF
2 CYS ATTN: N GAT
2 CYS ATTN: R N WAGNER

END

DATE

FILMED

3 — 88

DTIC